

RESPONSE OF FLEXIBLE PANELS TO TURBULENT

BOUNDARY LAYER EXCITATION

by

JAMES ALBERT MOORE

B.M.E., Rensselaer Polytechnic Institute (1967)

SUBMITTED IN PARTIAL FULFILLMENT

OF THE REQUIREMENTS FOR THE DEGREE OF

MASTER OF SCIENCE

at the

MASSACHUSETTS INSTITUTE OF TECHNOLOGY

September, 1969

Signature of Author.....
Signature redacted

Department of Mechanical Engineering, July 15, 1969

Certified by.....
Signature redacted

Thesis Advisor

Accepted by.....
Signature redacted

Chairman, Departmental Committee on Graduate Students



RESPONSE OF FLEXIBLE PANELS TO TURBULENT

BOUNDARY LAYER EXCITATION

by

James A. Moore

Submitted to the Department of Mechanical Engineering
on July 15, 1969, in partial fulfillment of the requirements for
the degree of Master of Science

ABSTRACT

The vibratory response of thin flexible panels excited by turbulent boundary layer pressure fluctuations is measured experimentally in order to investigate the effects of hydrodynamic coincidence on panel response. Experimentally determined cross correlations and cross spectral densities of the panel response are used to investigate the presence of travelling waves in the panel response in comparison with standing wave response. The various mechanisms for damping of panel response are examined. Values for radiation damping coefficients are experimentally evaluated and compared with analytically derived results. Values for purely mechanical damping coefficients are experimentally determined and compared with values for the total damping in the system that were determined from experiments involving the decay of energy in the panel. The radiation damping in air is shown to be negligible compared with the mechanical damping. The comparisons between damping values show acceptable agreement. Verification of the presence of convected wave patterns in the panel response is obtained only for limited test conditions.

Thesis Supervisor: Professor Patrick Leehey
Title: Professor of Naval Architecture and

TABLE OF CONTENTS

	<u>Page</u>
ABSTRACT	2
TABLE OF CONTENTS	3
ACKNOWLEDGMENTS	4
LIST OF FIGURES	5
GLOSSARY OF SYMBOLS	6
CHAPTER I - INTRODUCTION	8
CHAPTER II - EXPERIMENTAL PROCEDURE	17
CHAPTER III - EXPERIMENTAL RESULTS	23
CHAPTER IV - CONCLUSIONS	25
REFERENCES	33
APPENDIX I	35
APPENDIX II	39
APPENDIX III	42
FIGURES	43

ACKNOWLEDGMENTS

The author wishes to express his appreciation to Professor Patrick Leehey for his assistance and guidance in this thesis work. Appreciation is also given to the graduate students in the Acoustics and Vibration Laboratory for their assistance on problems of instrumentation. The author wishes to thank the National Science Foundation for fellowship assistance during the author's stay at M.I.T. This research was supported by the Naval Ship Research and Development Center through their General Hydromechanics Research Program. Funds were distributed out of M.I.T. through the Division of Sponsored Research under Contract Number N00014-67-A-0204-0002.

LIST OF FIGURES

<u>Number</u>	<u>Title</u>
1	Schematic of Wind Tunnel and Test Section
2	Photograph of Test Panel mounted in the Wind Tunnel Duct with the recording Apparatus in Place
3	Wall Pressure Spectral Density
4	Convection Velocities for the Turbulent Boundary Layer
5	Typical Plot of Velocity Spectral Density for the Panels
6	Sound Power Radiated Spectral Density
7	Plots of $R_{rad}(\omega)$, Experimental and Analytical Results
8	Energy Loss Factors
9	k Space Plot Showing Hydrodynamic Coincidence Semicircle
10	Broadband Cross Correlations
11	Cross Spectral Densities
12	Narrow Band Cross Correlations
13	Broadband Signal Levels, Mean Square Displacements

GLOSSARY OF SYMBOLS

C_a	Ambient speed of sound in air
C_L	Longitudinal speed of sound in steel
h	Panel thickness
k_a	Acoustic wave number, ω / C_a
k_m, k_n	Wave numbers in the direction of flow and perpendicular to the direction of flow
$k_{mn} = k_p$	$= (k_m^2 + k_n^2)^{1/2}$
L_1, L_3	Panel dimensions in the direction of flow and perpendicular to the direction of flow
M	Total mass of panel
$n_r(\omega)$	Reverberent room mode density
$n_s(\omega)$	Panel mode density
R_{mech}	Mechanical damping (lbm/sec)
R_{rad}	Radiation coefficient (lbm/sec)
$S_a(\omega)$	Panel acceleration spectrum, averaged over the area of the panel
$S_d(\omega)$	Panel displacement spectrum, averaged over the area of the panel
$\Phi_p(\omega)$	Sound pressure spectrum
$S_v(\omega)$	Panel velocity spectrum, averaged over the area of the panel
U_c	Convection velocity of pressure field in the turbulent boundary layer
V	Volume of the reverberant room
β_r	Energy decay constant for the reverberant room (sec^{-1})
\mathcal{K}	Radius of gyration of the panel
ρ_a	Ambient density of air
$(\sigma_{mn})_{avg}$	Dimensionless radiation coefficient for the panel averaged over the modes present in a 1/3 octave band

GLOSSARY OF SYMBOLS (cont.)

 $\mu(\omega)$

$$R_{\text{rad}} / (R_{\text{rad}} + R_{\text{mech}})$$

 η_s

Energy loss factor for the panel

CHAPTER I

INTRODUCTION

At a time when the trends in aerospace technology necessitate high speed lightweight vehicles with more complicated and delicate instrumentation, an understanding of the development of a noise environment in the vehicles as a result of pressure fluctuations in a turbulent boundary layer on the thin skin of the vehicle is important. It is important from the point of view of fatigue and vehicle operation by a human in the noise environment.

This thesis considered the vibratory response of thin panels to a turbulent boundary layer pressure excitation and the subsequent radiation of sound by the panels. The panel response was investigated in order to determine information concerning broadband and narrow-band convection velocities for travelling waves in the panel. The significance of travelling wave response in comparison with standing wave or normal mode response was considered. The panel response was also measured so that an experimental investigation of the mechanisms and levels of damping in the panel could be carried out. Radiation damping associated with an acoustic media facing the panel on one side was experimentally investigated. The purely mechanical damping through nonideal end supports and through losses internal to the panel was also experimentally measured.

An interesting phenomenon associated with the panel response to the strongly connected turbulent boundary layer pressure excitation is hydrodynamic coincidence. Turbulent boundary layer pressure

fluctuations are considered to be travelling waves of different frequencies where the convection velocities, U_c , are frequency dependent. As seen from Figure (4), the convection velocities are not significantly frequency dependent. A single representative value for the convection velocity was used to qualitatively describe the pressure excitation. When the spacial and temporal variations in pressure, as characterized by a wave number k and frequency ω match, the wave number in the direction of flow k_m and frequency ω , for the panel a resonance condition known as hydrodynamic coincidence exists. The region where hydrodynamic coincidence can exist for the panel is defined by a semicircle in k space of the functional form:

$$(k_m - U_c/2\chi C_L)^2 + k_n^2 = (U_c/2\chi C_L)^2$$

Maestrello has experimentally shown the presence of a convected wave pattern in the panel response whose connection velocity matches the convection velocity of the boundary layer pressure field. [1] The convected wave patterns are associated with hydrodynamically coincident response of the panel. It can be shown analytically that the presence of hydrodynamic coincidence leads to increased amplitudes of the modal forcing functions for the panel. [2] This analysis for the panel response follows a normal mode approach and while this approach predicts a stronger response for modes hydrodynamically coincident it does not indicate the presence of convected wave patterns. Cross correlation and cross spectral density techniques are used in an

attempt to obtain broadband and narrow band information concerning convection velocities in the panel vibratory response.

The second phase of the thesis dealing with damping was divided into two areas, one, the damping associated with radiation to an acoustic medium and two, with the purely mechanical damping. The radiation damping was investigated by experimentally evaluating radiation coefficients and comparing these with analytically derived coefficients. The mechanical damping was determined experimentally in a manner described further on and compared with values for the total damping determined from energy decay of panel response experiments. The total damping evaluated includes radiation effects which were shown experimentally to be negligible in comparison with the purely mechanical damping.

The analytical background for the radiation coefficient experiments has been done by Lyon and Maidanik.^[3] The derived result used in this experiment was:

$$\Phi_p(\omega) / S_a(\omega) = (\rho_a / c_a) (R_{rad} / \beta_r) (2\pi^2 \eta_r(\omega))^{-1}$$

The derivation of this expression involves the use of the concepts of statistical mechanics. A complete statement of the assumptions and restrictions present for the application of this expression to an experiment such as the radiation from thin panels excited by a turbulent boundary layer has been given by Leehey.^[4] A listing will be given here: It is assumed that the panels are lightly radiation loaded, such is the case for panels in air. The panel

modal excitations are assumed to be statistically independent and of band width greater than the effective band width of the corresponding uncoupled panel modal response. The modal excitation in this case relates to the pressure fluctuations in the boundary layer. The panel and acoustic field modal damping must be small and the gyroscopic radiation coupling must be small in comparison with either of these uncoupled modal damping values. In air with thin steel panels these restrictions are satisfied. The acoustic field must be reverberant and the panel vibratory field must also be reverberant or have only a single mode in the frequency band of interest. The modal densities for the panels used in these experiments have values yielding a minimum of approximately 10 modes in a 1/3 octave band with a center frequency of 200 cps for the thickest panel. There are approximately 22 room modes in this same 1/3 octave band. The number of modes per 1/3 octave band increases with frequency and with decreasing panel thickness. Only resonant interactions between acoustic and panel modes are considered in the analysis. Many modes in a frequency band allow for the assumption that the modal energies in the band are approximately equal if the modes in the band are lightly coupled through the presence of the acoustic medium.

The expression was further adapted taking into account the reverberant chamber. P. Leehey^[4] used the following relations:

$$\Phi_p(\omega) = (\rho_a c_a^2 / V \beta_r) \Pi_0(\omega)$$

and

$$\eta_r(\omega) = \omega^2 V / 2 \pi c_a^3$$

for the reverberant chamber to obtain the final result:

$$\Pi_0(\omega) = R_{rad}(\omega) S_V(\omega)$$

This expression was used to obtain the experimental values for $R_{rad}(\omega)$. Analytical values for the radiation coefficients were obtained by evaluating the following expressions:

$$(\sigma_{mn})_{avg} = (32 / \pi^3 A_p) (k_a^2 / k_p^3) (L_1 + L_3) \quad \text{for } k_a L_1, k_a L_3 < 3\pi$$

and

$$(\sigma_{mn})_{avg} = (32 / \pi^2 A_p) (k_a / k_p^3) + (4 / \pi A_p) (k_a^2 / k_p^2) (L_1 + L_3)$$

$$\text{for } k_a L_1, k_a L_3 > 3\pi$$

where

$$R_{rad} = \rho_a c_a A_p (\sigma_{mn})_{avg}$$

These expressions have been derived for acoustically slow modes, i.e., for $k_{mn} = k_p = (k_m^2 + k_n^2)^{1/2} \gg k_a$. It is seen from Appendix 4 and Figure (5) that the frequency range of significant panel response lies well below acoustic critical frequency and thus the resonant response of the panel is comprised of acoustically slow modes. Nonresonant contributions of acoustically coincident modes driven well above their resonant frequencies are taken to be negligible.

The expression for $k_a L_1, k_a L_3 < 3\pi$ was obtained for corner modes resonant in the frequency band $\Delta\omega$. For either or both $k_a L_1, k_a L_3 > 3\pi$ edge mode contributions are taken into account along with corner modes. These results were primarily derived by Maidanik [5] and modified by Davies [6] to include the frequency regime where the acoustic wavelength is comparable to the dimensions of the panel.

A method for the experimental determination of the mechanical damping was investigated. The purely mechanical damping, as distinguished from radiation damping, can be considered to arise from two possible sources. As damping implies a flow of energy from a system, vibration of the boundary of the panel would constitute a form of nondistributed damping. If the panel is considered to be mounted at its boundaries on an effectively infinite elastic foundation, there will be a flow of energy into the foundation at the boundary of the panel. It was noted experimentally that the level of vibration at the boundary was significantly smaller than a typical level of vibration for the boundary layer excited panels in the central region of the panel. The other source of damping would be a distributed form of damping occurring internally within the panel material.

The method involved the excitation of the panel by an acoustic field within the reverberant chamber surrounding the wind tunnel duct in which the panel was mounted. The resulting acceleration spectrum of panel response, $S_a(\omega)$, the excitation sound pressure spectrum, $\Phi_p(\omega)$, and previously determined experimental values for $R_{rad}(\omega)$, were used to determine the mechanical damping,

$R_{\text{mech}}(\omega)$, from the following equation, derived by Lyon and Maidanik [3]:

$$S_a(\omega) / \Phi_p(\omega) = \Gamma(\omega) \mathcal{M}(\omega)$$

where

$$\Gamma(\omega) = 2\pi (n_s(\omega) / M) (c_a / \rho_a)$$

and

$$\mathcal{M}(\omega) = R_{\text{rad}} / (R_{\text{rad}} + R_{\text{mech}})$$

R_{mech} is the only unknown in the above equation. The application of this expression to this test setup was contingent upon the satisfaction of the same restrictions as for the experiment to determine R_{rad} . Whereas before the turbulent boundary layer excitation was considered to be effectively white, now the speaker excitation of the reverberent acoustic field must be effectively white. The results were compared with damping values obtained from panel energy decay experiments involving 1/3 octave band filtered white noise excitations and decay in 1/3 octave bands. The reverberation times obtained from these energy decay experiments were used to calculate the energy loss factor .

For a single degree of freedom spring-mass-dashpot oscillator η , the energy loss factor, is defined as $R/\omega_0 M = \eta$. R is the constant of proportionality for the dashpot, M is the mass of the resonator and ω_0 is the resonant frequency for the system;

$$\omega_0' = (1 - 1/4 \eta^2)^{1/2} \omega_0 \quad . \quad \text{The short time average of the}$$

total energy in the system is $E = E_0 e^{-\gamma \omega_0 t}$ where E_0 is the initial energy for the natural or unforced vibrations.

Crandall^[7] considers a multimodal system where several modes have resonant frequencies lying in the frequency band of excitation. The excitation at $t=0$ is abruptly switched off and the decay response observed. The short time average total energy of a j^{th} mode after $t=0$ is shown to be given by:

$$U_j(t) = U_j(0) e^{-\beta_j t}$$

where β_j is a modal decay rate factor defined by $\beta_j = C_j / M$. M is the total mass of the system and C_j is a modal damping factor determined from $\int_{\bar{x}} C(\bar{x}) \psi_j(\bar{x}) \psi_k(\bar{x}) d\bar{x} = \delta_{jk} C_j$. $C(\bar{x})$ is the distributed damping coefficient for the system and appears in the differential equation for the system in the form $C(\bar{x}) \frac{\partial y(\bar{x}, t)}{\partial t}$,

where $y(\bar{x}, t)$ is the response being considered. $\psi_j(\bar{x})$ and $\psi_k(\bar{x})$ are orthogonal natural mode shapes for the system. For the panel $\psi_j(x_1, x_3) = (2/A_p) \sin k_m x_1 \sin k_n x_3$.

For the system response which is the sum of modal responses the initial decay rate of the short time average of total energy of the system is $\frac{dU}{dt} \Big|_{t=0} = - \sum_j \beta_j U_j(0)$

A weighted average of modal decay rates

$$\bar{\beta} = \sum_j \beta_j U_j(t=0) / \sum_j U_j(t=0)$$

is used to obtain the following result

$$\bar{\beta} = - \left(\frac{1}{U} \frac{dU}{dt} \right)_{t=0}$$

This relation was used to experimentally determine $\bar{\beta}$ for modes lying in a 1/3 octave band for the panels. $\bar{\beta}$ is related to the energy loss factor η by the following $\bar{\beta} = \omega_0 \eta$, where ω_0 is taken as the center frequency of the 1/3 octave band under consideration. For the case where many panel modes are resonantly excited by the 1/3 octave excitation, it was assumed that spacial variations in the decay rate $\bar{\beta}$ over the panel surface due to modal effects are negligible. It was also assumed that the short time average of the total energy of the system is proportional to the short time average of the squared displacement. This assumption was necessary as it was the decay of the short time average of squared displacement that was used experimentally to determine $\bar{\beta}$ and η .

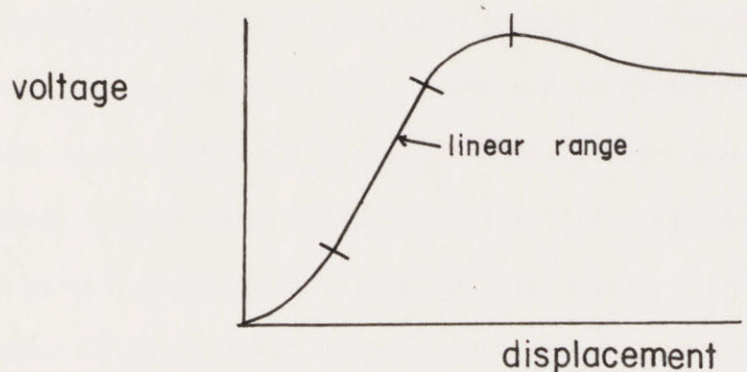
CHAPTER II

EXPERIMENTAL PROCEDURE

The object of the experimentation was to obtain directly values for the sound power radiated, $\Pi_0(\omega)$, and panel velocity spectrum, $S_v(\omega)$, for use in the calculation for the radiation coefficients, $R_{rad}(\omega)$.

Three test panels of surface dimensions $L_1=11"$, $L_3=13"$ and thicknesses .006", .003", .0015" were used. The panels were made of stainless steel shim stock marketed by Precision Brand, Inc. The panels were attached to aluminum frames using a commercial Ecco Bond epoxy. The panels and frames were flush mounted in the bottom wall of the wind tunnel ducting, a schematic of which is shown in Figure (|). Details concerning the wind tunnel can be found in a publication by C. Hanson.^[8] The turbulent boundary layer pressure fluctuations were created by mean flows in the center of the duct of 30 m/sec, 45m/sec, and 55m/sec. Panel displacement data in the form of an amplitude vs. time history was taken using a non-contacting optical displacement gauge, commercially known as the Fotonic Sensor, Model KD38 marketed by M.T.I. The gauge uses principles of fiber optics to shine a beam of light at a reflecting surface and to receive back the reflected light. The intensity of reflected light received back by the gauge is dependent upon the distance between the reflecting surface and the receiver tip. The reflected light received by the probe tips is transmitted through fibers to a photocell which transduces the light intensity to a

voltage signal proportional to the intensity. The overall characteristic of voltage output versus the distance between the probe tip and the reflecting surface looks like:



The level of the voltage output depends on the intensity of the light that is emitted from the transmitting fibers in the probe and the surface reflectivity, assuming that the surface is not optically diffuse. A section of the front portion of the characteristic curve is sufficiently linear and with sufficient sensitivity to be used to meter the panel response. The intensity of the transmitted light can be adjusted so that the value of the maximum voltage corresponds to a prescribed value, thus taking into account differences in surface reflectivity between the test surface and a surface used during the calibration procedure. The sensitivity of the characteristic curve for the test condition then corresponds to the sensitivity of the calibration characteristic curve. The averaged displacement of the panel vibration during test is adjusted so that the averaged voltage output lies in the middle of the linear range of characteristic curve. A.C. displacements of the panel then occur as oscillations about this D.C. set point.

The probe containing the light transmitting fibers and receiving

fibers was mounted in a traverse to allow for positioning on the surface of the panel. The traverse itself was attached to a rig resting on the floor. Two probes were used in the experimentation to provide concurrent time histories at two positions on the panel surface needed for cross-correlations and cross spectral densities. The electrical signals analogous to displacement were amplified using Ithaco low noise amplifiers, Model 225, and recorded on two channels of a four channel Precision Instrument tape recorder, Model 6200. A photograph of the panel, sensing and recording apparatus is shown in Figure (2).

A signal to noise ratio check was undertaken to insure that the data recording technique was sensitive enough to accurately record the panel displacement. The signal to noise ratio check was performed by assembling the recording apparatus in a manner identically as for actual test conditions. The B & K analyzing apparatus was used to determine signal levels in 1/3 octave bands for the case where the panel was not excited by a turbulent boundary layer. The worst condition for S/N developed for the thickest panel at the lowest flow speed where S/N was approximately 10db at the highest recorded frequency. For other frequencies S/N improves and reaches a maximum of near 40 db. For other test conditions and frequencies a value for S/N of 15 db appears to be a minimum limiting value. It was concluded that the recording apparatus was sensitive enough to provide accurate records.

As the velocity spectral density needed for the calculations is a quantity averaged over the area of the panel, displacement levels

at various points on the panel surface were measured. Time histories for the two probes were recorded for longitudinal probe separations of .375", .8", and 1.2". The probes were located in the central region of the panel for these measurements. The displacement of the panel at the boundaries is very nearly zero. Signal levels in 1/3 octave bands will also be zero at the boundaries. The manner in which these levels go to zero was determined experimentally by measuring the displacement at various positions near the boundaries.

It was determined experimentally that the panel velocity signal levels in 1/3 octave frequency bands are essentially constant over the central region of the panel. The drop off in level at the boundaries was sharp. This result depends upon a high panel mode density where individual modal variations across the panel are buried amongst the response of the many other modes in the 1/3 octave band. The average over the panel of the velocity spectral levels was determined using an averaged value for the central region modified by what was assumed to be a linear drop off in level at the boundaries.

Sound pressure and sound power levels in 1/3 octave frequency band width were measured by H. Davies^[6] for the same test conditions as existed for the experimental results presented in this paper.

The 1/3 octave band displacement spectral levels were produced using continuous time histories provided by tape loops made from the recorded data. A B & K frequency analyzer, Model 2105, and Graphic Level Recorder, Model 2305, were used in conjunction with B & K 1/3 octave stepping filters to produce the spectral plots. The velocity

spectral levels were obtained by multiplying the displacement spectral levels by ω_0^2 , ω_0 being the 1/3 octave band center frequency. The spectral density of velocity response of the panel was determined by dividing the spectral level by the bandwidth.

For the acoustic field excitation experiment a speaker was placed in the reverberant chamber surrounding the tunnel duct in which the panel was mounted. A white noise generator and MacIntosch 40 watt amplifier were used to drive the speaker. The resulting spectral density of panel displacement was obtained as before, and the acceleration spectral levels in 1/3 octave bands obtained by multiplying by ω_0^4 . Sound pressure signals were obtained by using the B & K equipment as before. The resulting values for mechanical damping were compared with values obtained from energy decay in experiments performed by the author and H. Davies. Energy loss factors in 1/3 octave bands for the three panels used were obtained by mounting the panels in the wind tunnel duct and exciting them using an electromagnet. The excitation through the electromagnet was 1/3 octave band filtered white noise provided by a B & K Random Noise Generator Model 1402. The excitation was cut and the "reverberation" time for the decay of panel displacement signal was measured in the appropriate 1/3 octave band using the B & K frequency analyzer and graphic level recorder. Energy loss factors were then computed from the reverberation times. These experiments were performed on the panels for test cases where there was a mean flow in the tunnel duct. The electromagnetic excitation was therefore superimposed upon the turbulent boundary layer pressure excitation. The decay of the response of the

panel due to the electromagnet was measured; the response due to turbulence remaining.

In using an electromagnet as an excitation it must be noted that the mechanical force exerted on the panel is proportional to $|\sin \omega t|$ where $\sin \omega t$ is the electronic signal input to the electromagnet. The force then contains a D.C. component, a component at (2ω) and high harmonics of lesser significance. This can be shown by evaluating a Fourier series for $|\sin \omega t|$. There is no component at (ω) . This was the reason for filtering the panel response in a 1/3 octave band an octave higher than the 1/3 octave input to the electromagnet. The decay of panel response due to the higher harmonics was not of interest.

Cross correlations for the panel displacement data were obtained using a Par signal correlation, Model 100. Cross spectral densities of panel displacement were obtained using Spectral Dynamics tracking filters of 50 Hz bandwidth, Model SD101A, driven by a Spectral Dynamics sweep oscillator, Model SD104A-5. The coincident and quadrature components were obtained from a Spectral Dynamics CO-Quad Analyzer, Model SD109A. Graphical plots of the coincident and quadrature spectra were obtained as continuous functions of frequency on an X-Y plotter. In conjunction with the efforts to demonstrate the presence of travelling waves, the .0015" thick panel was narrowed transversely to a width of 4" and data for longitudinal probe separations of .375", .8" and 1.2" for flow speeds of 30 m/sec, 45 m/sec, and 55 m/sec was obtained. The cross spectral densities are normalized against the square root of the product of the power spectral densities of the individual signals from the two probes.

CHAPTER III
EXPERIMENTAL RESULTS

Spectral levels, in 1/3 octave bands, of panel response averaged over the area of the panel were determined by considering that the spectral levels in the central region of the panel were essentially constant and that near the boundaries the spectral levels decreased linearly from a representative average level over the central region to zero at the boundaries. The average over the panel of spectral levels would then be equal to the product of the representative average level for the central region and the ratio $A_{\text{eff}}/A_{\text{panel}}$. A_{eff} is approximately equal to 1/2 times the area of the region of the panel near the boundaries where the spectral levels are assumed to decrease linearly, added to the area of the central region of the panel where the spectral levels are essentially constant. The dividing line between the two regions of spacial variation of spectral levels of panel response was experimentally determined. The transition between regions was marked. Spectral levels in the central region varied by approximately 2 or 3 db over the region. The accuracy of this technique was sufficient for its intended purpose. Low S/N ratios for reduced signal levels at the boundaries prevented a more definitive interpretation of the drop off. Values for $A_{\text{eff}}/A_{\text{panel}}$ lie near .9. A typical plot of $S_V(\omega)$ is given in Figure (5). A plot of the radiated sound power is given in Figure (6). Analytical and experimental results for R_{rad} are found in Figure (7). Damping values for the panels in 1/3 octave bands are found in Figure (8). The results of the experiment where the panel was acoustically excited

are added to the plot for the .006" panel. The values of $S_d(\omega)$ averaged over the panel area, used to determine R_{mech} , were determined in the same way as for $S_v(\omega)$ using an average value for $A_{\text{eff}}/A_{\text{panel}}$ for the same panel thickness.

A k-space plot showing the location of the resonant coincident panel modes along a semicircle is shown in Figure (9). Cross correlation curves are shown in Figure (10). Cross spectral density plots are presented in Figure (11). Narrow band cross correlations are shown in Figure (12).

CHAPTER IV

CONCLUSIONS

Cross correlation and cross spectral density plots were obtained to yield information concerning convected wave patterns in the panel displacement response. If convection is present in the signals a cross correlation will in general be an uneven function of time delay. The major peak will appear shifted from $\tau = 0$ to a value $\tau = \tau_0$. An autocorrelation of a random signal has its maximum value at $\tau = 0$. If we consider two random signals identical except that one is delayed in time by s_0 / u_c , a cross correlation viewed about $\tau_0 = s_0 / u_c$ will appear as an autocorrelation. The maximum value will occur at τ_0 , the time delay between the two signals.

A broadband convection velocity could then be defined by the ratio s_0 / τ_0 where s_0 is the separation between positions where the panel signal is being cross correlated. Maestrello^[1] has presented experimental results where the broadband convection velocity determined from s_0 / τ_0 matches the corresponding broadband convection velocity of the turbulent boundary layer pressure field which is exciting the panel. Cross correlations of data from this research work do not reveal dominating convection patterns in the panel response. For the 11" by 13" panels, convected patterns in cross correlations are found for the thinnest panel (.0015") at a flow speed of 55 m/sec and probe separation of 1.2". Convection is found in the downstream direction and less definitely in the upstream direction. For smaller probe separations the presence of convection is less discernable.

For the other panels convection was not apparent in the cross correlations of panel displacement response.

Cross correlations for the narrowed panel reveal a more dominant convection pattern for convection in the downstream direction. The presence of convection in the upstream direction, as before, is less certain. Narrowing the panel in the lateral x_3 direction has the effect of increasing the spacings between modes in the k_3 direction in k space by approximately a factor of three in this case (i.e., from 13" wide to 4" side). This would significantly decrease the number of panel modes resonantly excited by the boundary layer pressure. It would not affect that part of the panel response for which the panel appears infinite, that is, the convected or travelling wave response. The effects of both responses are formally represented in the series expansions in panel eigenfunctions for the response. Associating the travelling wave response for which the panel appears infinite with the effects of hydrodynamic coincidence one sees that this travelling wave response will not be affected by altering the panel dimensions. It will therefore be of greater significance in comparison with the reduced resonant modal response. Cross correlations of the total response would then show stronger travelling wave or convection effects. This agrees with the comparison between results for the 13" wide and 4" wide panels. It would also explain the dominate effects of convection obtained for Maestrello's experimental results. The resonant mode density for the panel used by Maestrello was approximately 1/16 the value for the .0015" by 11" by 13" panel used in these experiments.

For both the 13" wide and 4" wide panels at 55 m/sec, the downstream broadband convection velocities were approximately

250 ft/sec. The broadband Convection velocity associated with the pressure field was 120 ft/sec corresponding to a free stream velocity in the tunnel duct of 180 ft/sec. This value for the panel response was nearly twice what would be expected. This might be interpreted to mean that the convected response for these limited circumstances is not strongly associated with hydrodynamic coincidence, in that the spacial and temporal variations in the convected panel response and the pressure fluctuations do not match. It is necessary to distinguish between convected panel response, for which the panel appears infinite, and panel response that is spacially defined by the panel mode shapes. Hydrodynamic coincidence strongly affects the standing wave response as well as being thought of as directly relating to the convected panel response, It is possible that the presence of the significant standing wave response is affecting the locations of the peaks of experimental cross correlations and that the convection is actually associated with hydrodynamic coincidence.

The cross spectral density is essentially the Fourier transform of the cross correlation:

$$\phi(x_1^1, x_3^2, x_1^2, x_3^1, \omega) = \frac{1}{2\pi} \int_{-\infty}^{\infty} R(x_1^1, x_3^2, x_1^2, x_3^1, \tau) e^{-i\omega\tau} d\tau$$

If $R(, , , ,)$ is a combination of even and odd functions, its product with $e^{-i\omega\tau}$ will involve real and imaginary components which are combinations of even and odd functions. $\phi(, , , ,)$ will have both real and imaginary components which are the integrals over the even parts of the real and imaginary components of the integrand. For cross correlations where the maximum value is shifted from $\tau = 0$, this is exactly the case and the corresponding spectral density will have both real and imaginary components.

If the shift in the maximum of the cross correlation from $\tau = 0$ is associated with convection effects it then follows that the presence of the quadrature component is also associated with convection effects. The experimental determination of the coincident and quadrature components of cross spectral density involve the use of two phase matched narrow band filters. These do not exist in reality and the result of the actual phase mismatch between filters is to give a value for the quadrature component on the order of 15% of the coincident component for test signals where the quadrature component should be zero, that is, when there is a zero degree phase difference between the test signals. There is a great deal of uncertainty involved with the interpretation of cross spectral plots as a result of this instrumental error.

Narrow band convection velocities are obtained from cross spectral densities by assuming that the phase information of the cross spectral density is contained in a factor of the form $e^{i\omega x/U_c}$. Other dependencies on lateral and longitudinal separation would be real and would constitute an amplitude factor. This functional form parallels a form used in describing the turbulent boundary layer pressure field and is presumably valid where the signal is strongly dominated by convection, as is the case with the turbulent boundary layer. Its application to the panel response becomes obscured as the response of the panel is not dominated by convection effects; on the contrary, the experiments tend to show that the opposite is true for the panels used in this experimentation.

If this method is applied for the 11" by 4" by .0015" panel at 45 m/sec at a probe separation of 1.2" where the quadrature component appears to be significant in comparison with possible in-

strumental errors one finds that the narrow band convection velocity obtained is 119 ft/sec at 2400 cps. The turbulent pressure field at 2400 cps is convected at 99 ft/sec. This result more closely approximates the expected result though the panel narrow band convection velocity is still significantly higher than expected. It is to be noted that this is a single isolated data point. In general the cross spectral density plots do not have significant quadrature levels and therefore do not reveal the presence of convection in the panel response.

Narrow band filtering of the two displacement signals and a cross correlation of the filtered outputs provides a check on the cross spectral density plots obtained. The coincident spectral value at a frequency ω_0 , the center frequency of the narrow band filter, corresponds to the $\tau = 0$ value of the narrow band cross correlation. The quadrature spectral value at frequency ω_0 corresponds to the value of the narrow band cross correlation at $\tau = \pi / 2 \omega_0$. The experimental results obtained agree with the cross spectral densities and did not alter the conclusions concerning narrow band convections in the panel response.

The agreement between the analytically determined and experimentally determined radiation coefficients is within 5 db for the most part. The most notable deviations occur with the thinnest panel at the highest flow speeds. The experimental curve lies significantly above the analytical result. In the higher frequency regions of the curves the experimental results appear to drop off sharply. An explanation for this is not known. A factor which might

affect the experimental results has to do with the presence of a static pressure differential across the panel. The differential is due to the presence of flow in the tunnel duct on one side of the panel. An attempt was made to reduce this differential but residual leakage between the chamber surrounding the duct and the outside maintained a pressure differential across the panel sufficient to cause deflections at the center of the panel on the order of a few panel thicknesses or more. If the pressure differential is significantly large, membrane effects in the panel will become of importance. A membrane term will have to be added to the differential equation for the panel. An attempt to determine the order of magnitude of these effects and their dependence on the panel thickness and the magnitude of the pressure difference is carried out in Appendix I. The results indicate that a pressure differential across the plate will decrease the value for k_p at a given frequency. In determining the magnitude of the effect, it was initially assumed that the value of the tensile stress at the center of the panel was representative of a constant value for the whole panel. The actual solution for the additional membrane term is much more complicated, involving the tensile stress as a function of position. The value for the tensile stress of the center is too high a value to use, it is the maximum value on the panel. It is seen from Appendix I that the effect of tension at 1000 cps adds approximately 16.4 db to the analytical result for R_{rad} for the .0015" thick panel at 55 m/sec. This value is too great as a result of the simplifying assumption that the tensile stress is spacially constant. A lower value would

correspond better with the experimental deviations. An approximate method taking account of spacial variations in tensile stress would add only 1.43 db at 1000 cps to the analytical result.

As a result of this analysis the presence of a pressure differential across the panel is a plausible explanation as to why the experimental values lie significantly above the analytical results, though an exact analytical correction is not available. It is seen from Appendix I that the effects of tensioning increase with increasing pressure differential (i.e., flow speed) and decreasing panel thickness. The relative significance of the bending and shear stress term and the membrane term is such that for higher values of k_p the bending and shear stress term is of greater importance. The membrane term is proportional to k_p^2 while the bending and shear stress term is proportional to k_p^4 . As ω monotonically increases with k_p for resonant situations, the membrane or tension effects are less important at higher frequencies. Excluding the unexplained marked drop off of the experimental radiation coefficient at higher frequencies the deviations above the analytical result diminish with increasing frequency being most significant at the lowest frequency considered. The experimental results show trends much like these for the two thinner panels at the two higher flow speeds.

Values for R_{mech} determined from the experiment where the panel was acoustically excited are presented in Figure (8a). It is to be noted that for 1/3 octave center frequencies other than 315, 400, and 500, the signal to noise ratios of the panel displacement signal are less than 5 db; for these points, values of 9 or 10 db for S/N exist.

The results of the energy decay experiments are presented in Figure (8). For the thicker panels (.006", .003") the results for different flow speeds and pressure differentials across the panels converge within approxiamately 2 db. For the .00]5" panel the results at zero flow speed differ significantly from those taken with a mean flow over the panel. The results at flow appear to converge within approxiamately 2 db. This discrepancy may be explained with reference to the static pressure differential that existed across the panel. The decay of panel response to the electromagnetic excitation may have been affected in two ways as a result of this pressure difference. The pressure differential tensions the panel and this may have caused a stronger coupling of the panel to the support frame at the boundaries; thus providing for a greater flow of energy from the panel through the non-ideal boundaries. The pressure differential also causes a static deflection of the panel. It is conceivable that a significantly stronger interaction of the panel with the turbulent boundary layer as a result of the static deflection allowed for a flow of energy from the panel to the flow when the electromagnetic excitation was removed. It was experimentally noted that the static deflection of the .00]5" panel was significantly greater than for the other two panels. This could be because the thinness of the panel made it difficult to mount the panel properly in the support frame. The damping measured is the total damping of the coupled panel and acoustic system. In air the radiation damping is small and we can compare the total damping with the purely mechanical damping obtained from the acoustic excitation experiment. The comparison provides an acceptable agreement.

REFERENCES

1. Maestrello, L., "Use of Turbulent Model to Calculate the Vibration and Radiation Response of a Panel with Practical Suggestions for Reducing Sound Level", J. Sound & Vib., 1967, 5 (3), p. 407-488.
2. Lin, Y. K., Probabilistic Theory of Structural Dynamics, McGraw-Hill Book Co., New York, 1967, Chapter 7.
3. Lyon, R. and Maidanik, G., "Power Flow Between Linearly Coupled Oscillators," J. Acous. Soc. Am., 1962, 34 (5), p. 623.
4. Leehey, Patrick, "Trends in Boundary Layer Noise Research," presented at the AFOSR-UTIAS Symposium on Aerodynamic Noise, University of Toronto, May, 1968.
5. Maidanik, G., "Response of Ribbed Panels to Reverberant Acoustic Fields," JASA 34, 809, 1962.
6. Davies, H., "Sound from Turbulent Boundary Layer Excited Panels," M.I.T. Acoustics and Vibration Laboratory Report No. 70208-2, 1969.
7. Crandall, Stephen, "Random Vibration of Interconnected Systems," presented at the 11th Mid-Western Mechanics Conference, Iowa State University, August, 1969.
8. Hanson, Carl, "The Design and Construction of a Low Noise, Low Turbulence Wind Tunnel," M.I.T. Acoustics and Vibration Laboratory Report 796]]-], January, 1969.
9. Timoshenko, Woinowsky, and Krieger, Theory of Plates and Shells, McGraw-Hill Book Co., New York, 1959, 2nd Edition, p. 424.
10. Blake, William, "Turbulent Boundary Layer Wall Pressure Fluctuations on Smooth and Rough Walls," M.I.T. Acoustics and Vibration

10. Laboratory Report No. 70208-1, January, 1969.
11. Bendat and Piersol, Measurement and Analysis of Random Data, John Wiley and Sons, Inc., New York, 1966, Chapter 6.
12. Dyer, I., "Sound Radiation into a Closed Space from Boundary Layer Turbulence", Second Symposium on Naval Hydrodynamics, ONR/ACR-38, 1958.

APPENDIX I

EFFECTS OF TENSION ON THE MEMBRANE TERM IN THE DIFFERENTIAL EQUATION

The fact that the static deflection at the center of the panel was large necessitates a large deflection analysis. A reference for this analysis is found in Timoshenko, The Theory of Plate and Shells. [9] The approximate analysis considers the static deflections of a clamped square plate under a uniform load q_0 . The dimensions of the square panel are $2a$ by $2a$ by h .

The load q_0 is considered to be the sum $q_1 + q_2$, in such a manner that q_1 is balanced by the bending and shearing stresses from the theory of small deflections, the part q_2 being balanced by membrane stresses.

The deflection at the center for the theory of small deflections is

$$w_0 = 0.73q_1a^4/Eh^3$$

where q_1 becomes

$$q_1 = w_0Eh^3/0.73a^4$$

The deflection for a membrane is

$$w_0 = 0.802a(q_2a/Eh)^{1/3} \quad \text{from which}$$

$$q_2 = w_0^3 Eh/0.516a^4$$

The deflection w_0 is found from

$$q = q_1 + q_2 = w_0 E h^3 (1.37 + 1.94 w_0^2 / h^2) / d^4$$

where q is a known variable, the static pressure difference across the panel.

For a flow speed of 55 m/sec the pressure differential q is equal to 4.54 cm of H_2O or 6.45×10^{-2} psi. The corresponding values for 30 m/sec and 45 m/sec are .826 cm of H_2O and 2.48 cm of H_2O respectively. Assuming the following values for the constants:

$$E = 3 \times 10^7 \text{ psi}, \quad h = 3.38 \times 10^9 \text{ in}^3, \quad d = 6 \text{ in}$$

for the .0015" thick panel, the expression for q becomes:

$$6.45 \times 10^{-2} \text{ psi} = 7.81 \times 10^{-5} \text{ psi } W_0 (1.37 + 8.63 \times 10^5 W_0^2 / \text{in}^2) / \text{in}$$

A solution to this is $W_0 = 9.85 \times 10^{-2} \text{ in}$; there was only one real root. The corresponding loads q_1 and q_2 are $q_1 = 1.05 \times 10^{-5} \text{ psi}$ and $q_2 = 6.43 \times 10^{-2} \text{ psi}$. It is seen that the small deflections term is negligible in comparison with the membrane term. The tensile stress level at the middle of the panel due to the membrane term is

$$\sigma_2 = 0.616 E W_0^2 / d^2 \quad \text{and evaluated is } \sigma_2 = 4.98 \times 10^3 \text{ psi}$$

If we now consider that the tensile stress σ is constant across the panel the added membrane term to the differential equation becomes:

$$c_m^2 \nabla^2 w \quad \text{where } c_m^2 = s / \mu$$

β is the tension per unit length and μ is the mass per unit area.

$$s = \sigma_2 \times h \quad \text{and} \quad \mu = .28 \frac{\text{lbm}}{\text{in}^3} h \quad ; \quad \text{evaluating } c_m^2 :$$

$$c_m^2 = 6.86 \times 10^6 \text{ in}^2 / \text{sec}^2$$

The dispersion relation for the panel becomes $(\chi c_L)^2 k_p^4 + c_m^2 k_p^2 = \omega^2$.

For the .0015" thick panel $\chi c_L = 88.5 \text{ in}^2 / \text{sec}$ and the

$$\text{dispersion relation becomes } 8.05 \times 10^3 \text{ in}^4 k_p^4 + 6.86 \times 10^6 \text{ in}^2 k_p^2 = \omega^2.$$

A general expression for c_m^2 would be:

$$c_m^2 = 1.41 (q^2 E d^2 / h^2)^{1/3}$$

A ratio of c_m^2 to $(\chi c_L)^2$ would become:

$$c_m^2 / (\chi c_L)^2 = q^{2/3} / h^{4/3}$$

From this we would expect the magnitude of the tension effects to be greatest at the higher flow speed (i.e., higher q 's) and thinner panels.

As the dependencies involves k_p raised to different powers the membrane term will become less significant with higher values for k_p .

Using the previously derived dispersion relation to calculate the effect of a pressure differential for 55 m/sec on the .0015" panel at 1000 cps we obtain the following results: without the membrane term $k_p = 8.34 \text{ in}^{-1}$; and, with the membrane term $k_p = 2.35 \text{ in}^{-1}$.

In the analytical expression for R_{rad} , k_p appears as $1/k_p^3$. The reduction in k_p due to membrane effects would mean a 44 fold increase in the calculated value for R_{rad} for this particular case. On a db scale this would be 16.4 db.

If the variations in tensile stress over the panel are taken

into account in an approximate way, the following result is obtained:

$$\omega = (\chi c_L) (k_p^2 + 5\pi^2/64 a^2 (w_0/h)^2 k_p)$$

where the assumption is made that this result for a square of side a can be applied to a panel of dimensions 11" by 13".

Evaluating this expression for k_p at 1000 cps where a is taken to be 12" and w_0 is the previously calculated deflection in the middle of the panel, k_p becomes 7.57×10^{-1} inches. This would add 1.46 db to the analytical result for R_{rad} at 1000 cps. This is a significant change in the calculated effect of tension.

APPENDIX II

CROSS SPECTRAL DENSITY OF PANEL DISPLACEMENT RESPONSE

BASED ON A NORMAL MODE APPROACH

The basis for this approach was taken from a text by Y. K.

Lin. [3] The results are presented here:

$$\Phi(x_1, x_3, x'_1, x'_3, \omega) = \sum_{mno} \sum_{p} \Psi_{mn}(x_1, x_3) \Psi_{op}(x'_1, x'_3) H_{mn}(\omega) H_{op}(\omega) I_{mnop}(\omega)$$

$\Phi(\omega)$ is the cross spectral density of panel response. $\Psi_{mn}(\)$ and $\Psi_{op}(\)$ are orthogonal natural mode shapes for the panel.

$$\Psi_{mn}(x_1, x_3) = (2/\sqrt{A_p}) (\sin m\pi x_1/L_1) (\sin n\pi x_3/L_3)$$

$H_{mn}(\omega)$ is the modal response function taking into account fluid loading effects on one side of the panel. These are taken into account through an added mass term, γ_{mn} , and an acoustic or radiation damping term, σ_{2mn} ,

$$H_{mn}(\omega) = \left(D \left(k_{mn}^4 - \frac{m_p \omega^2}{D} \left(1 + \frac{\rho_a c_a}{\omega m_p} \gamma_{mn} \right) + i \left(\frac{m_p \omega^2}{D} \right) \eta_s \operatorname{sgn} \omega + \frac{m_p \omega^2}{D} \frac{\rho_a c_a}{\omega m_p} \sigma_{mn} \right) \right)$$

m_p is the mass per unit area of the panel and D is the flexural rigidity for the panel.

$$I_{mnop}(\omega) = \int_0^{L_1} dx_1 \int_0^{L_1} dx'_1 \int_0^{L_3} dx_3 \int_0^{L_3} dx'_3 \Phi_{pp}(x_1, x_3, x'_1, x'_3, \omega) \Psi_{mn}(\) \Psi_{op}(\)$$

$\Phi_{pp}(\)$ is the cross spectral density of the turbulent pressure field.

Using a Corco's model to approximate experimental cross correlations;

$$\Phi_{pp}(\omega) = \Phi_p(\omega) B\left(\frac{r_3 \omega}{U_c}\right) A\left(\frac{r_1 \omega}{U_c}\right) e^{-i \frac{r_1 \omega}{U_c}}$$

where $r_1 = x'_1 - x_1$ and $r_3 = x'_3 - x_3$. The functions $A(\)$ and $B(\)$ may be approximated as exponentials of the forms

$$B(\) = e^{-\frac{|r_3| \omega}{U_c \alpha_3}}$$

and

$$A(\) = e^{-\frac{\omega |r_1|}{U_c \alpha_1}}$$

For the test conditions used in these experiments, Blake in his doctoral thesis has shown experimentally that $\alpha_3 = 1.1$ and $\alpha_1 = 8$. [10]

[12]

If a Dyer criterion is applied and it is assumed that cross modal terms are negligible $I_{mn}(\omega)$ becomes:

$$I_{mn}(\omega) = \Phi_p(\omega) \left(\frac{\beta_1^2}{(k_m - \frac{\omega}{U_c})^2 + \beta_1^2} + \frac{\beta_2^2}{(k_m + \frac{\omega}{U_c})^2 + \beta_2^2} \right) \left(\frac{\beta_3}{k_n^2 + \beta_3^2} \right)$$

where $\beta_1 = \omega / \alpha_1 U_c$ and $\beta_3 = \omega / \alpha_3 U_c$. The cross spectral density of panel displacement responses then becomes:

$$\phi(\) = \sum_m \sum_n \Psi_{mn}(x_1, x_3) \Psi_{mn}(x'_1, x'_3) |H_{mn}(\omega)|^2 I_{mn}(\omega)$$

which is a real number. The application of a Dyer criterion to this normal mode result drops out the quadrature component of the cross

spectral density and therefore does not analytically predict the presence of convected wave patterns in the panel response.

APPENDIX III

PARAMETERS OF THE PANEL AND TURBULENT BOUNDARY LAYER

1. Panel Dispersion Relation

$$k_p^2 = \omega / \chi c_L$$

$h = .006''$	$\chi c_L = 2.456 \text{ ft}^2/\text{sec}$
$h = .003''$	$\chi c_L = 1.228 \text{ ft}^2/\text{sec}$
$h = .0015''$	$\chi c_L = 0.614 \text{ ft}^2/\text{sec}$

2. Panel Mode Density

$$n_s(\omega) = A_p / 4\pi \chi c_L$$

$h = .006''$	$n_s(\omega) = .03225 \text{ sec}$
$h = .003''$	$n_s(\omega) = .0645 \text{ sec}$
$h = .0015''$	$n_s(\omega) = .129 \text{ sec}$

3. Pressure Field Convection Velocities

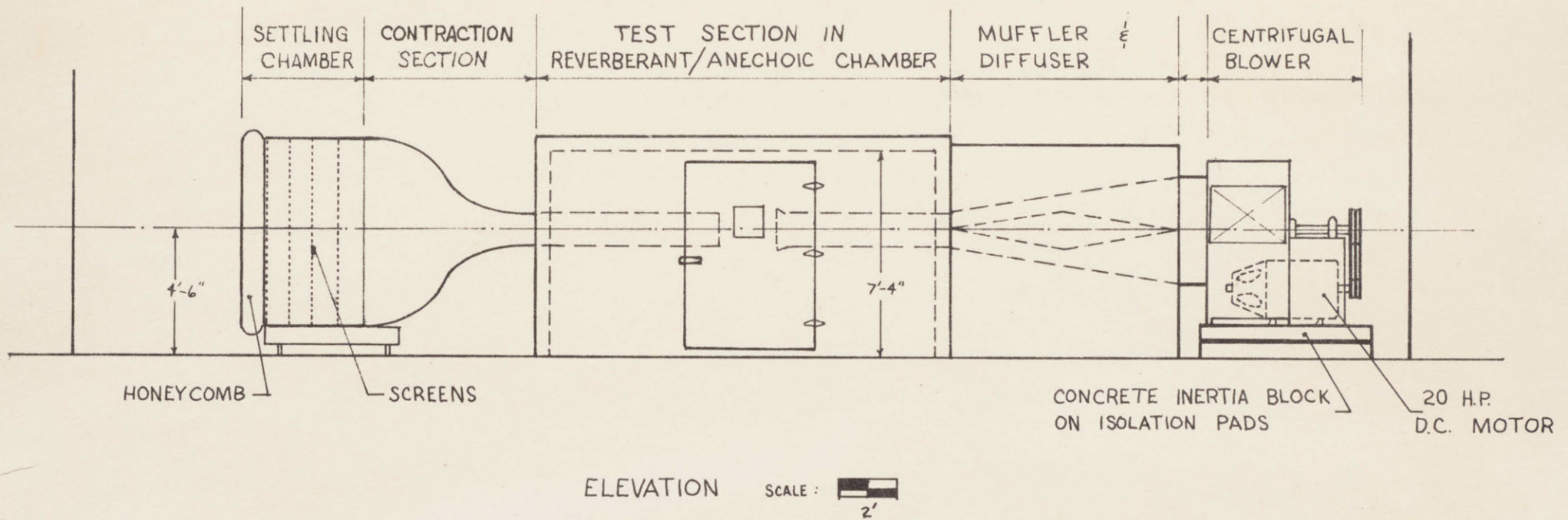
U_∞	U_c
180.4 ft/sec	120 ft/sec
147.6 ft/sec	99 ft/sec
98.4 ft/sec	63 ft/sec

Values obtained from Blake's doctoral thesis

4. Acoustic Critical frequency

$$\omega_c = 78000 \text{ cps}$$

FIGURES



GENERAL SPECIFICATIONS:
 CONTRACTION RATIO : 20 : 1
 TEST SECTION : 15" x 15" SQUARE , OPEN OR CLOSED

Fig. 1a

WIND TUNNEL FACILITY - ROOM 5-024
 ACOUSTICS & VIBRATIONS LABORATORY
 MASSACHUSETTS INSTITUTE OF TECHNOLOGY
 CEH 8-23-66

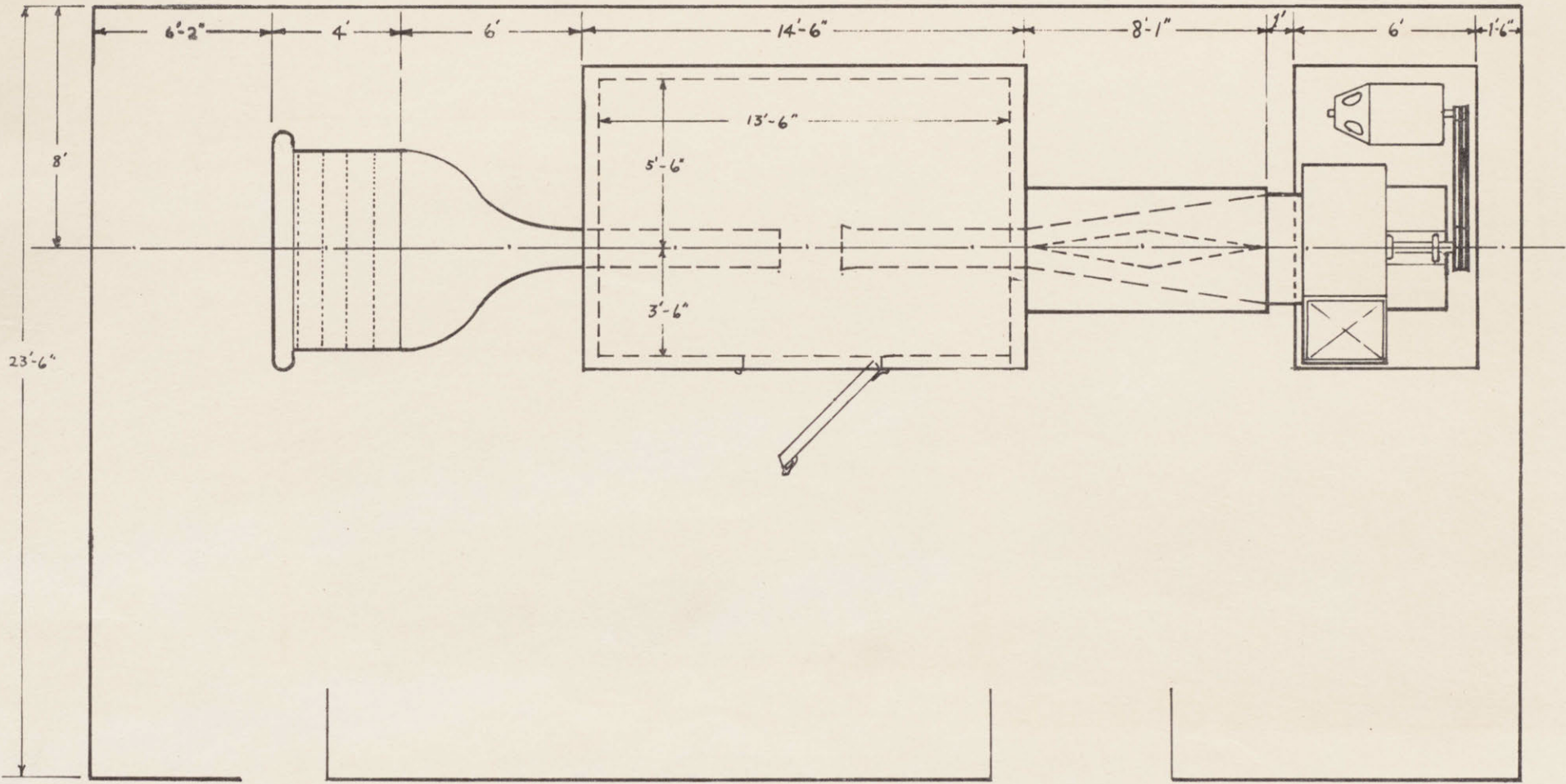


Fig. 1b PLAN VIEW SCALE :  2'

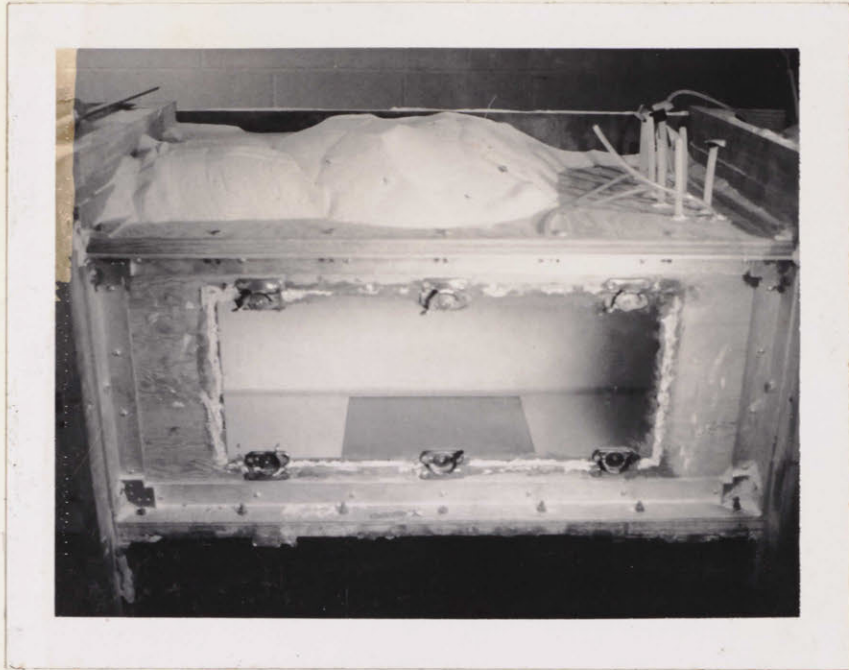
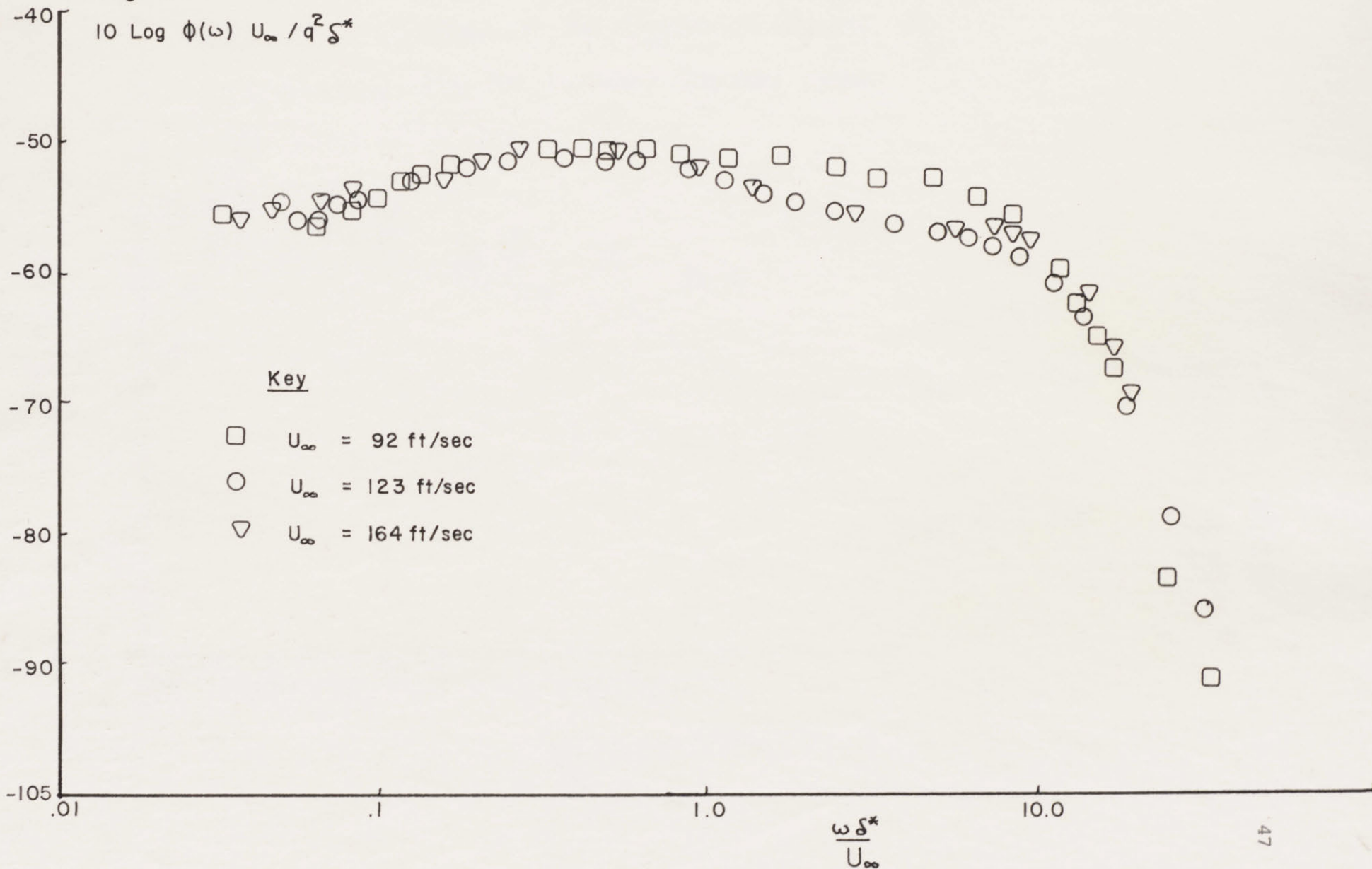


Fig.2 Photographs of Test Panel in the Wind Tunnel
with Recording Apparatus

Fig. 3

Wall Pressure Spectral Density



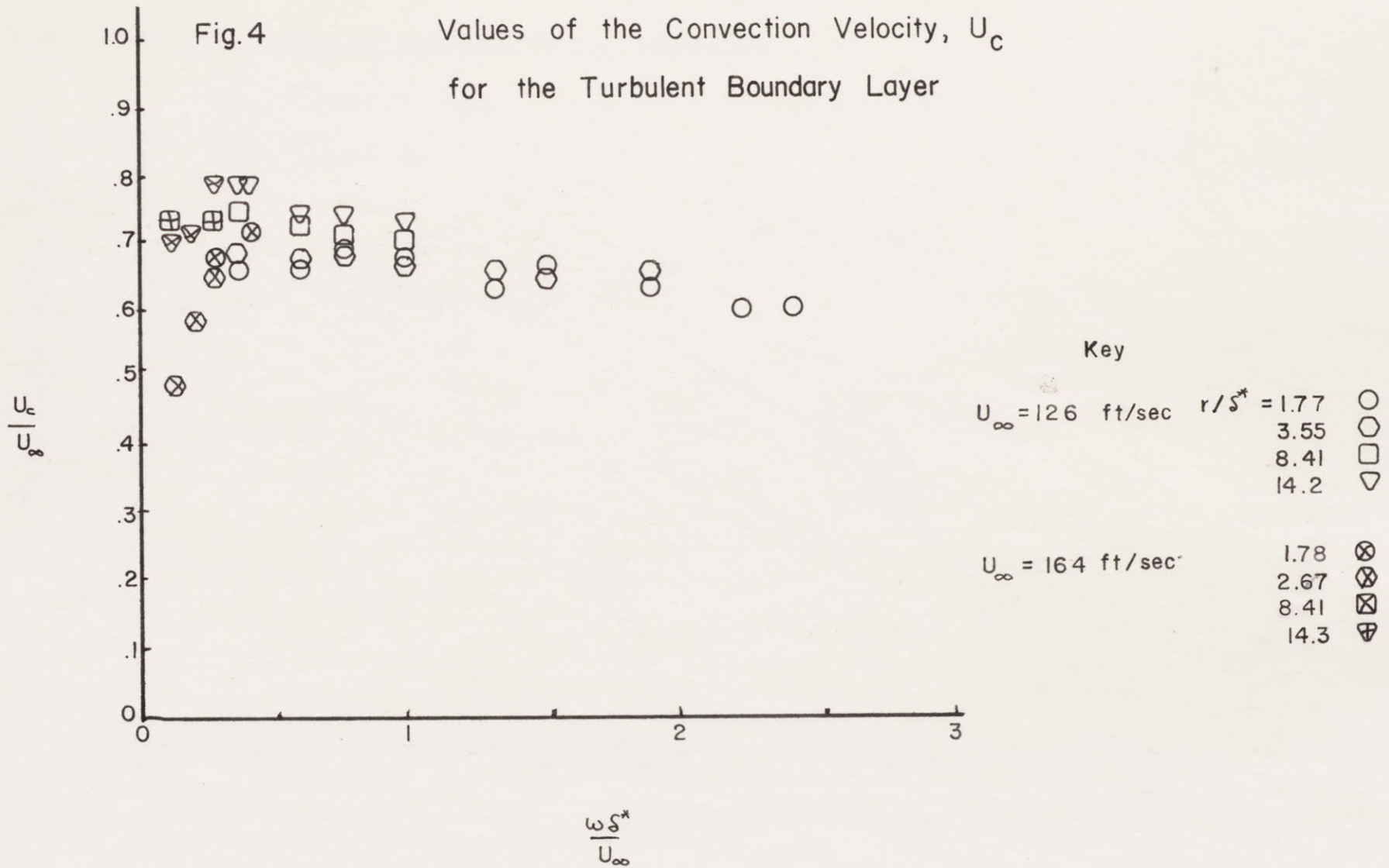


Fig. 5 Panel Velocity Spectra $S_V(\omega)$ ($\text{in}^2/\text{sec}^2\text{hz}$)

panel thickness .003"

flow speed 45 m/sec

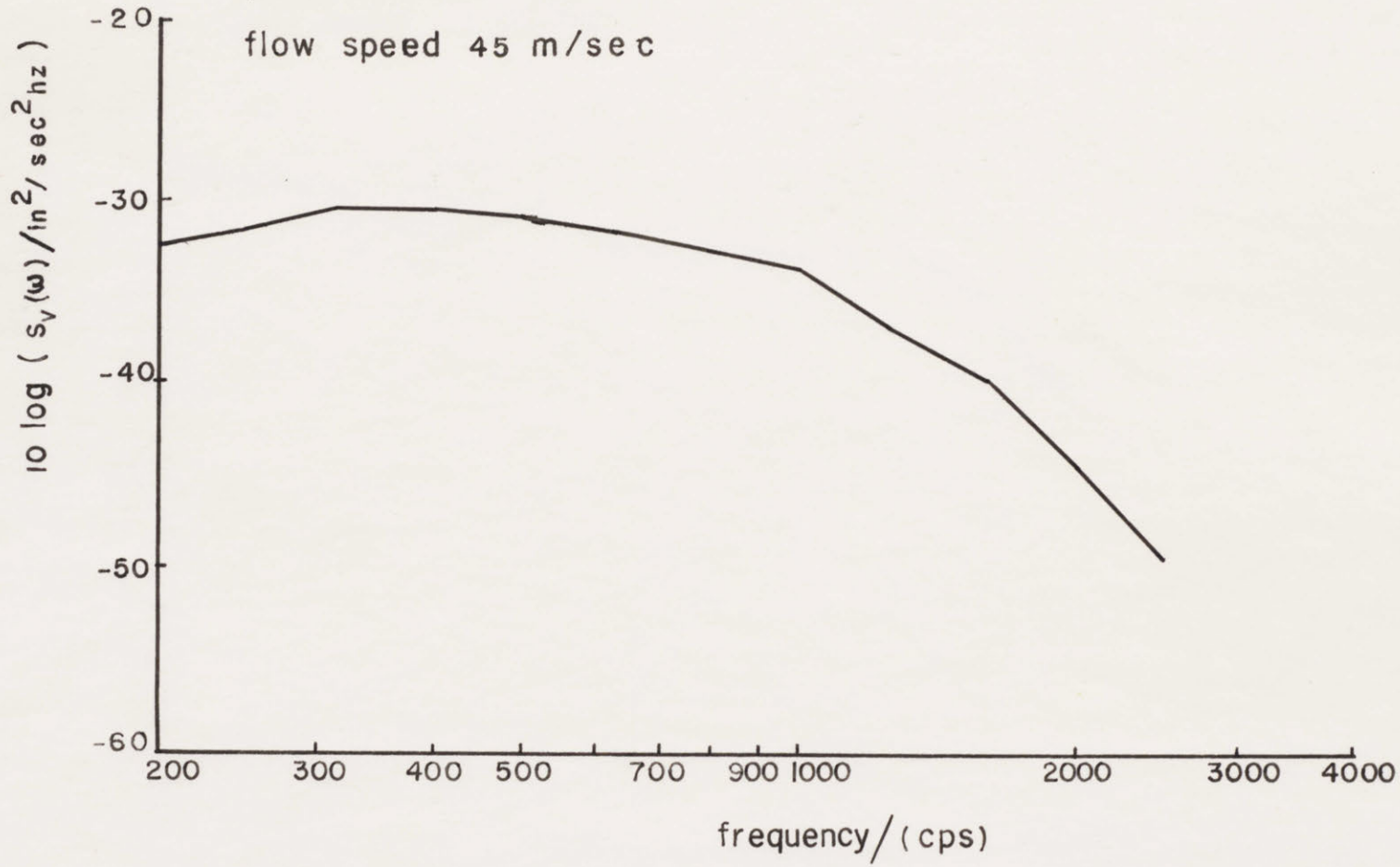


Fig. 6

$\Pi_o(\omega)$ Sound Power Radiated
panel thickness .003"
flow speed 45 m/sec

$10 \log (\Pi_o(\omega) / \text{watts/hz})$

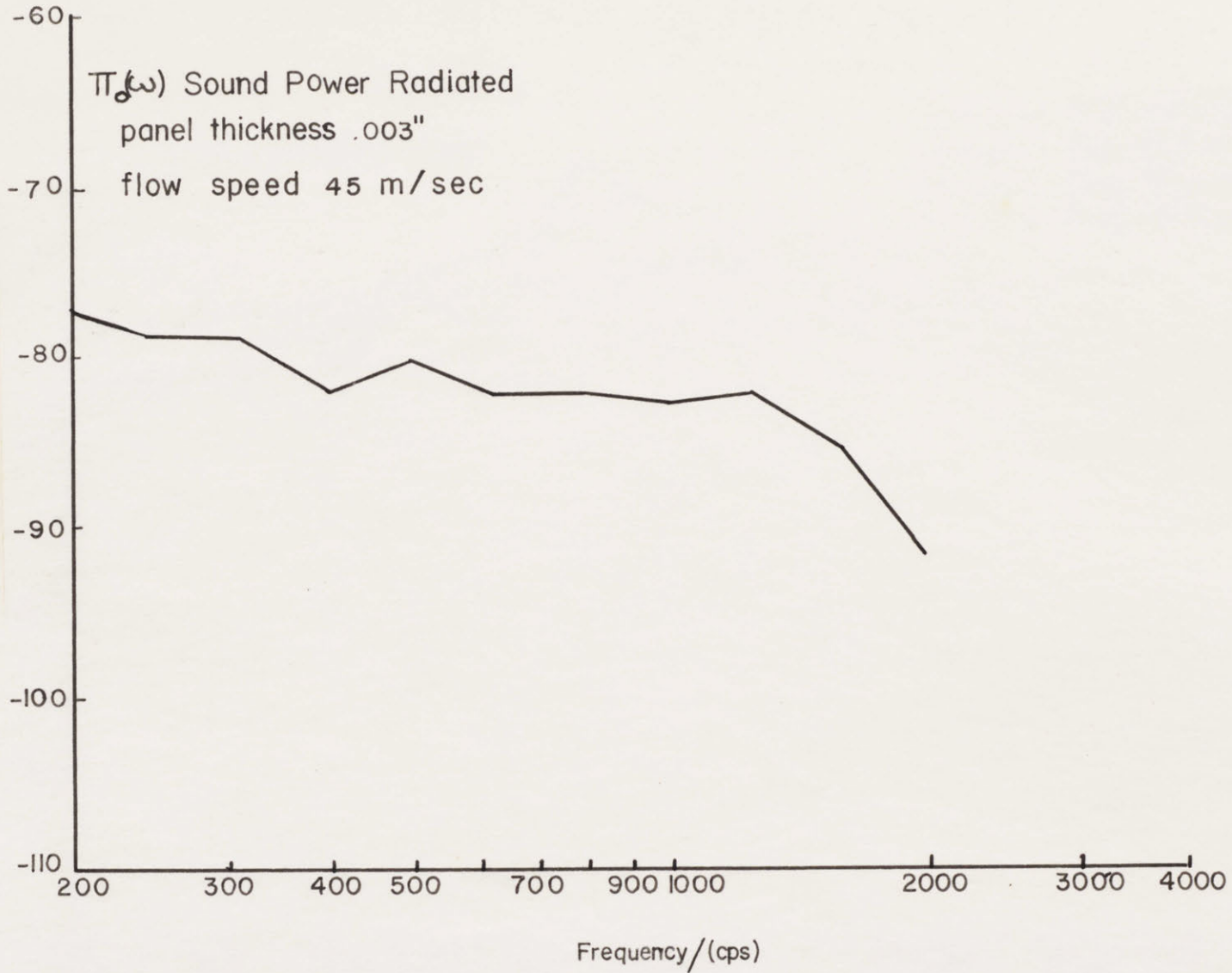


Fig. 7a

$R_{rad}(\omega)$ vs Frequency
panel thickness .006"

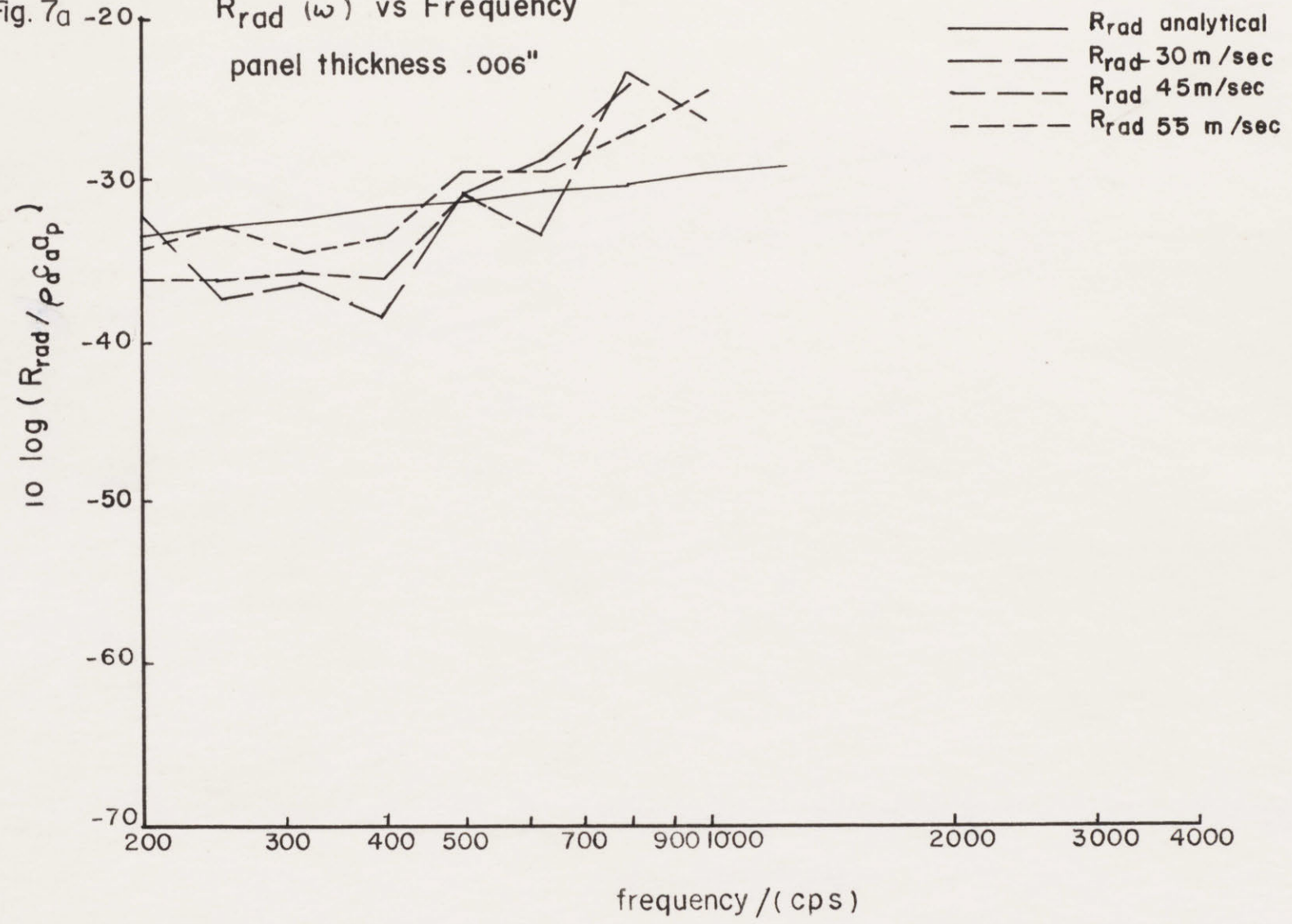


Fig.7b

$R_{rad}(\omega)$ vs Frequency
panel thickness .003"

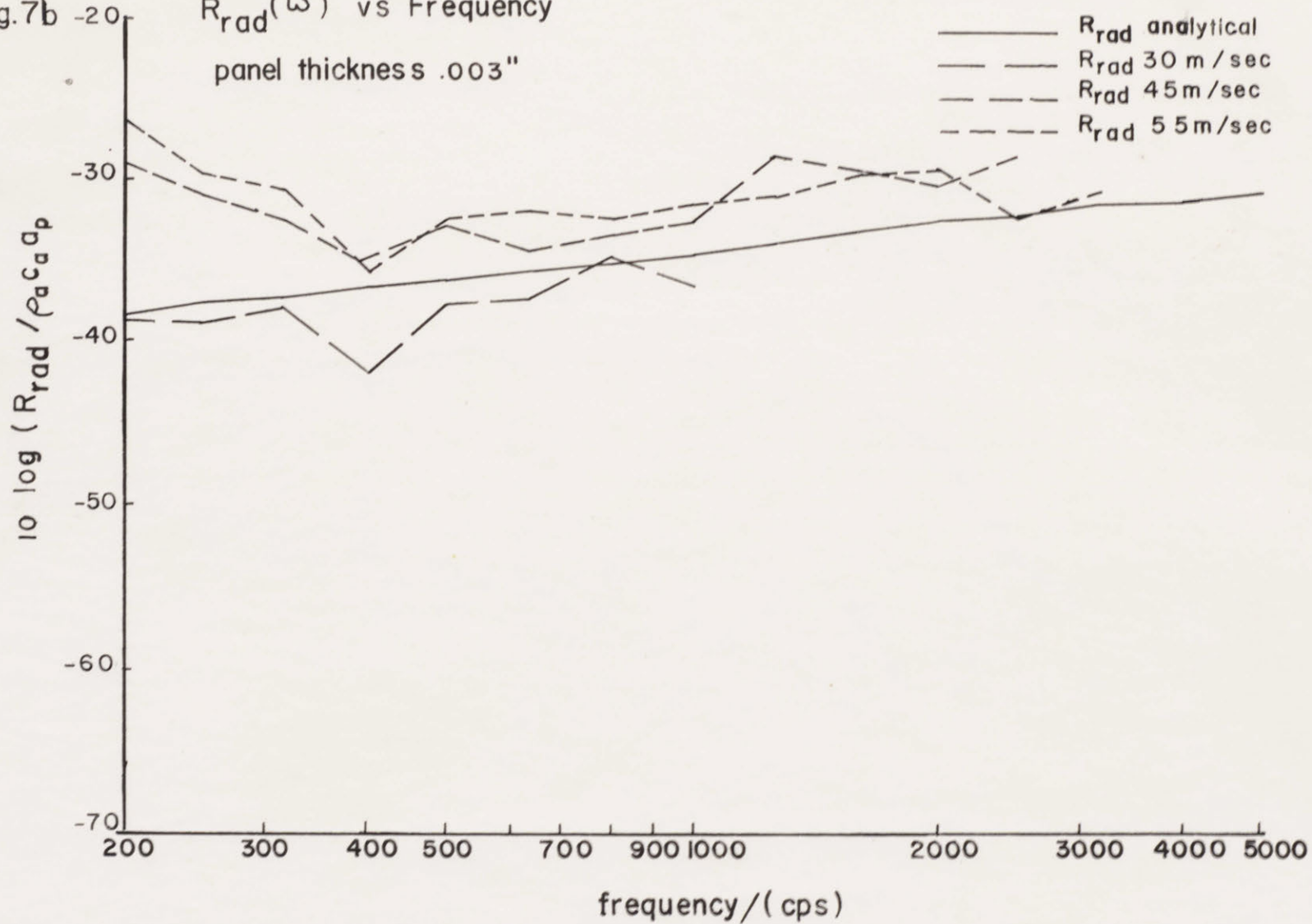


Fig.7c

$R_{rad}(\omega)$ vs Frequency

panel thickness .0015"

- R_{rad} analytical
- - - R_{rad} 30 m/sec
- · - R_{rad} 45 m/sec
- - - R_{rad} 55 m/sec

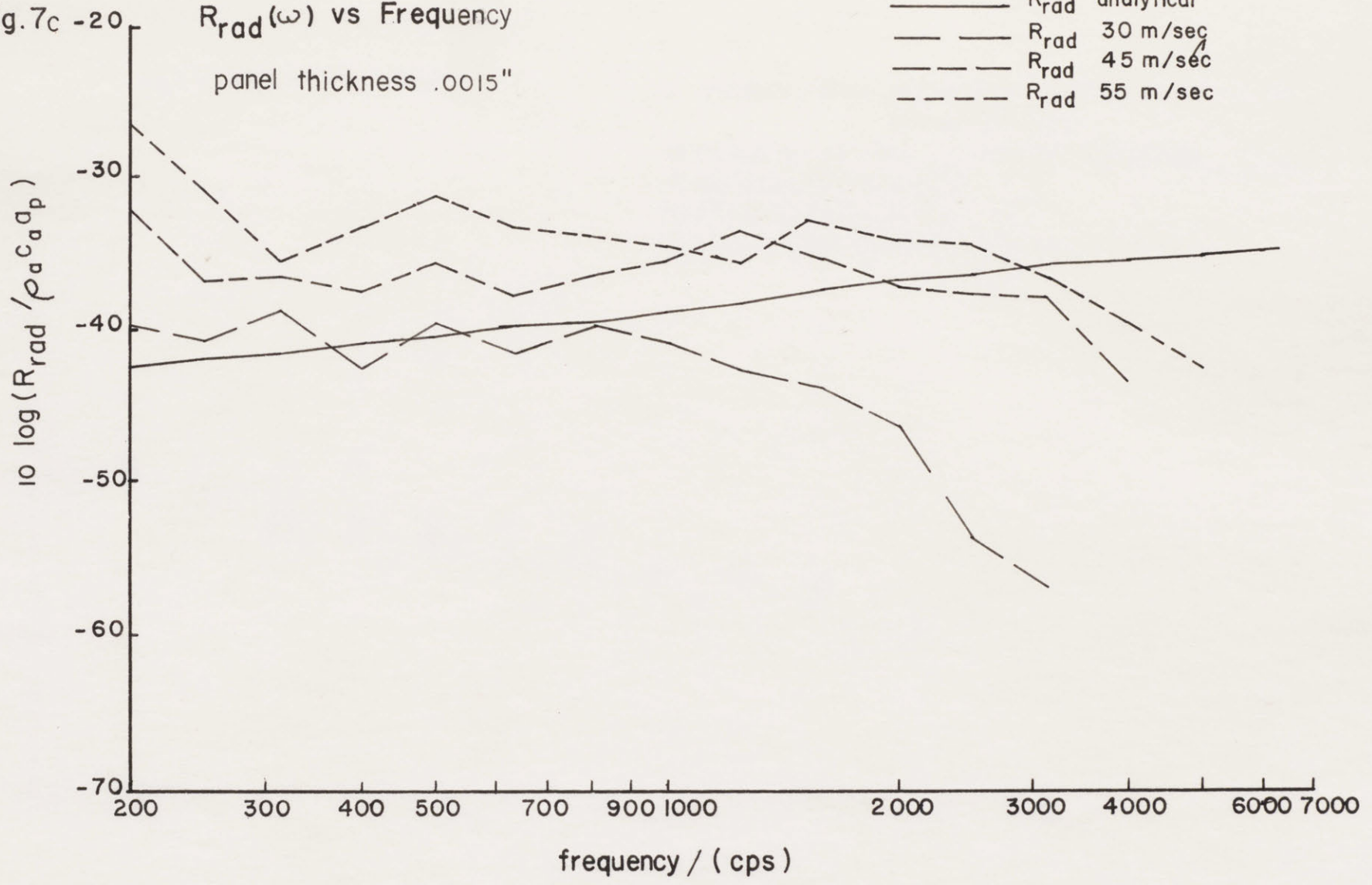


Fig. 8a Energy Loss Factor (η)

panel thickness .006"

- × 0 m/sec 0 cm H₂O pressure differential across the panel
- ▽ 30 m/sec .826 cm H₂O pressure differential
- 45 m/sec 2.48 cm H₂O " "
- 55 m/sec 4.54 cm H₂O " "
- results from speaker excitation of the panel

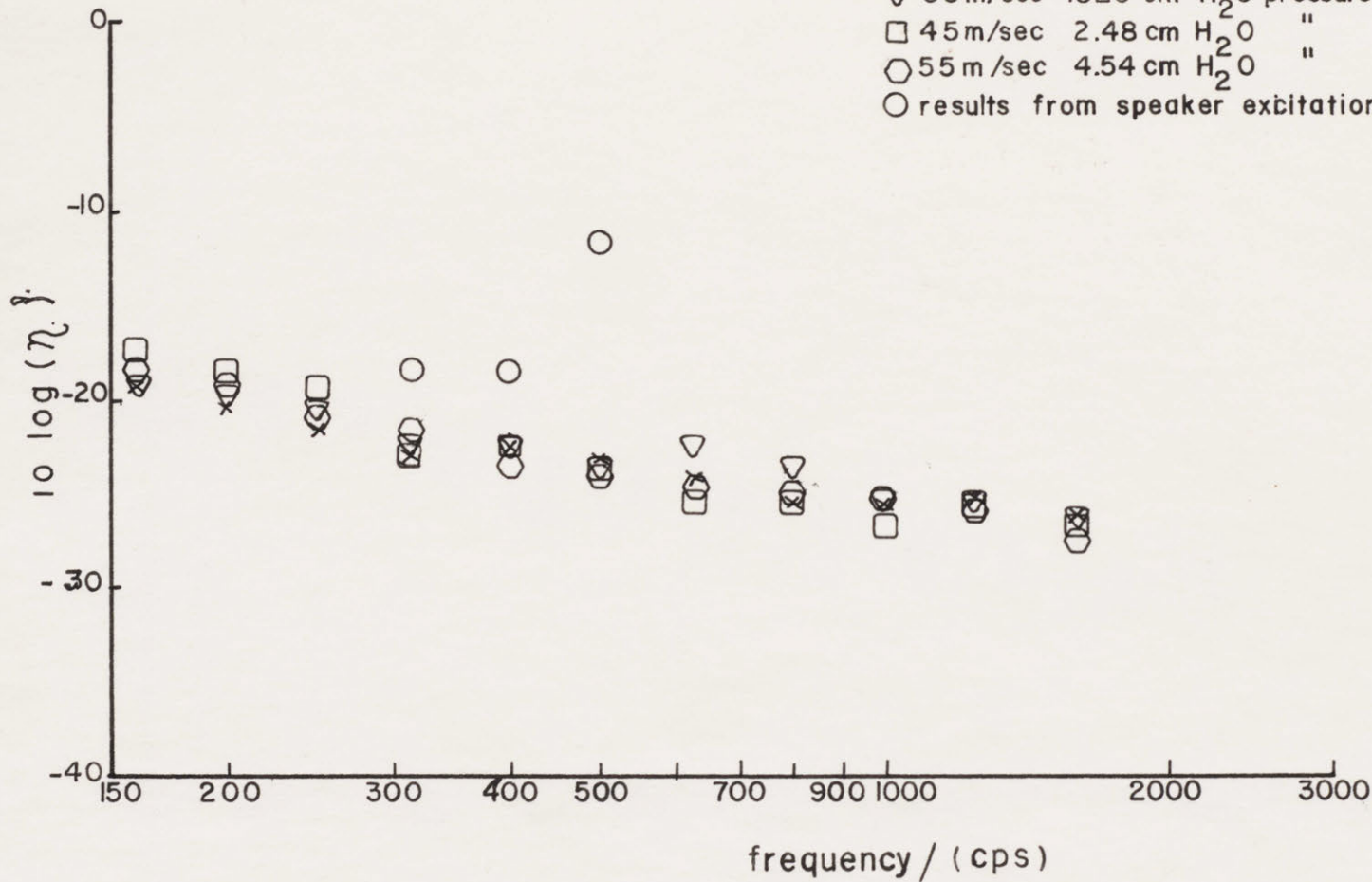


Fig. 8b Energy Loss Factor (η)
panel thickness .003"

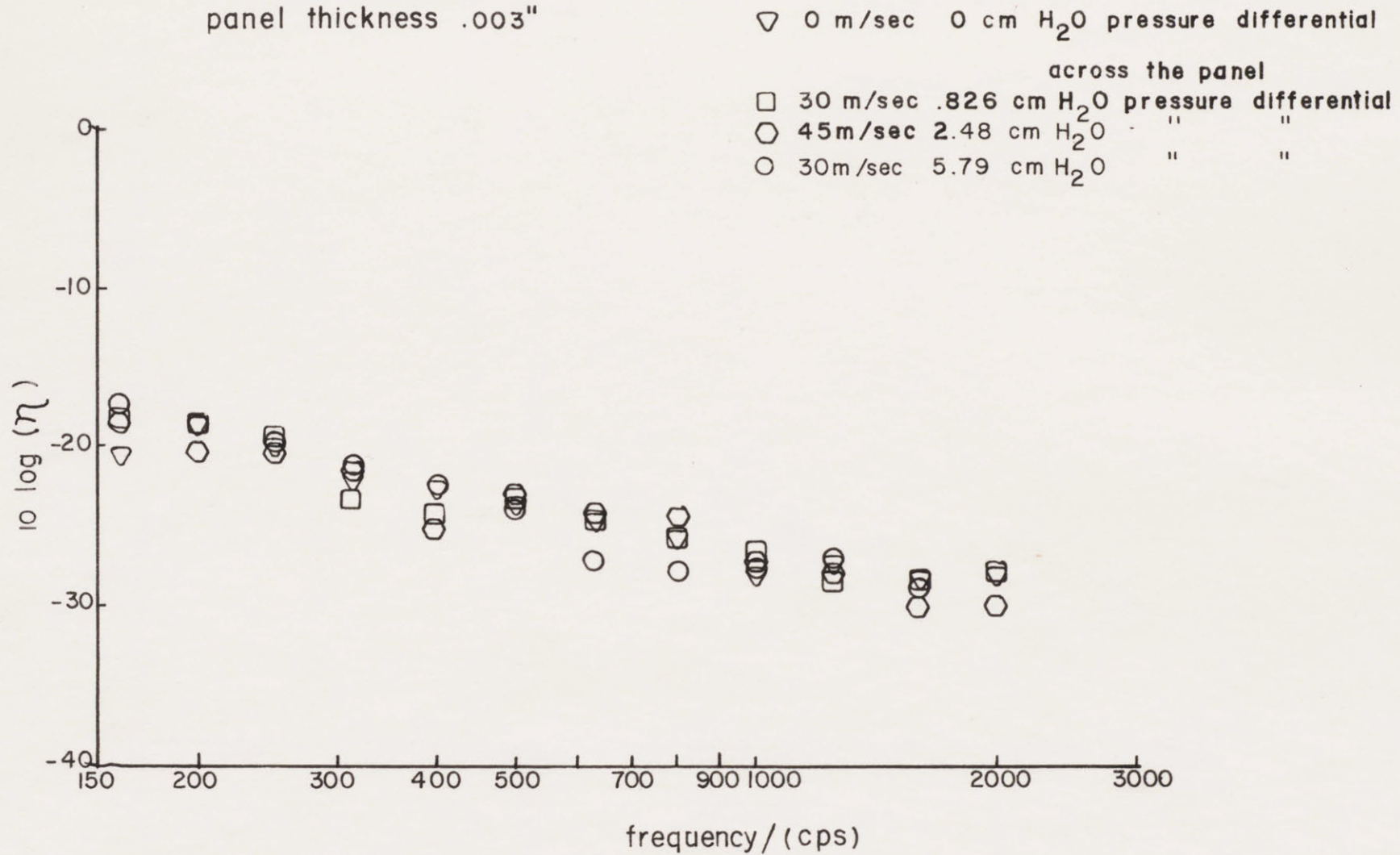


Fig. 8c

Energy Loss Factor (η)

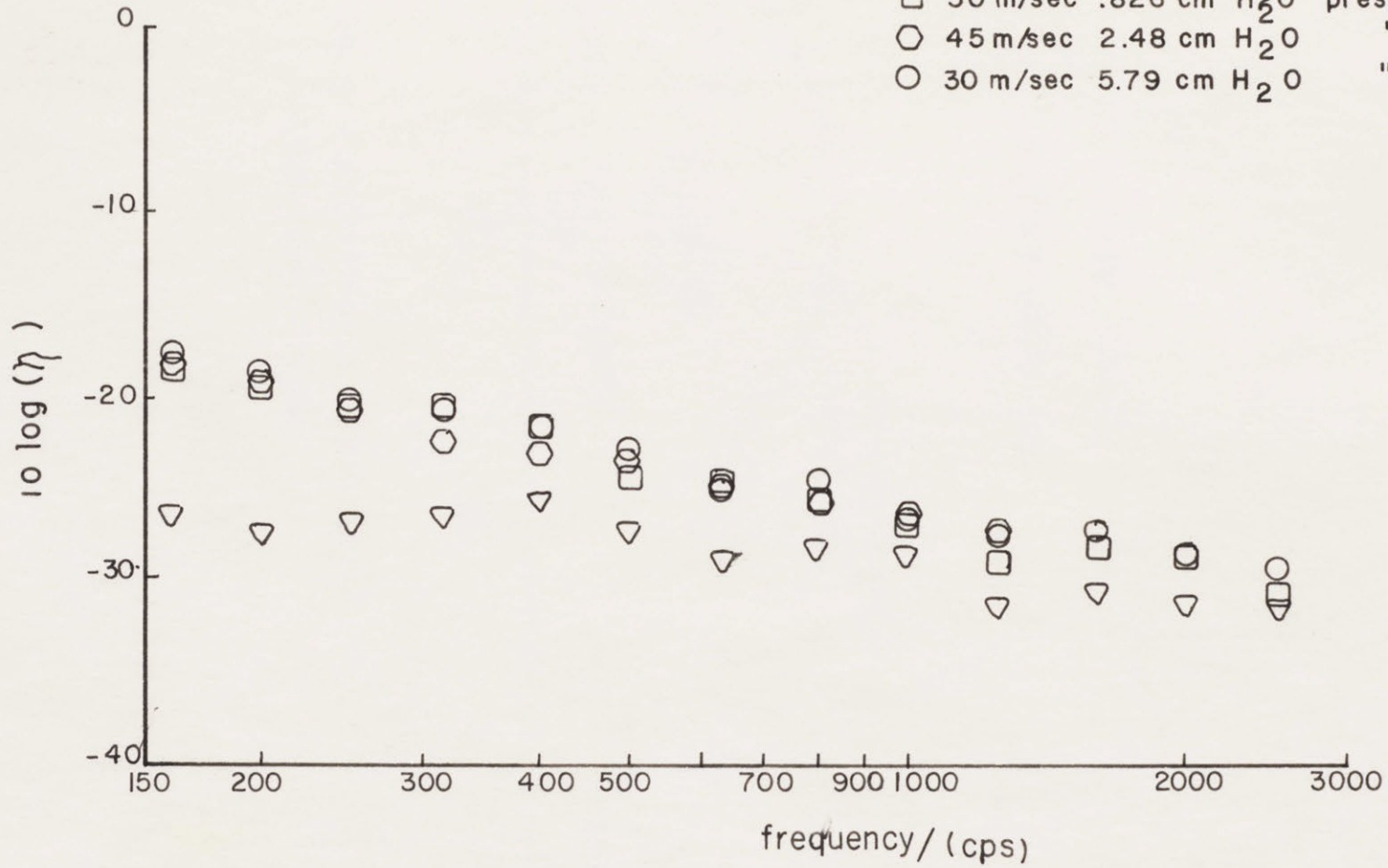
panel thickness .0015"

▽ 0 m/sec 0 cm H₂O pressure differential across the panel

□ 30 m/sec .826 cm H₂O pressure differential

○ 45 m/sec 2.48 cm H₂O " "

○ 30 m/sec 5.79 cm H₂O " "



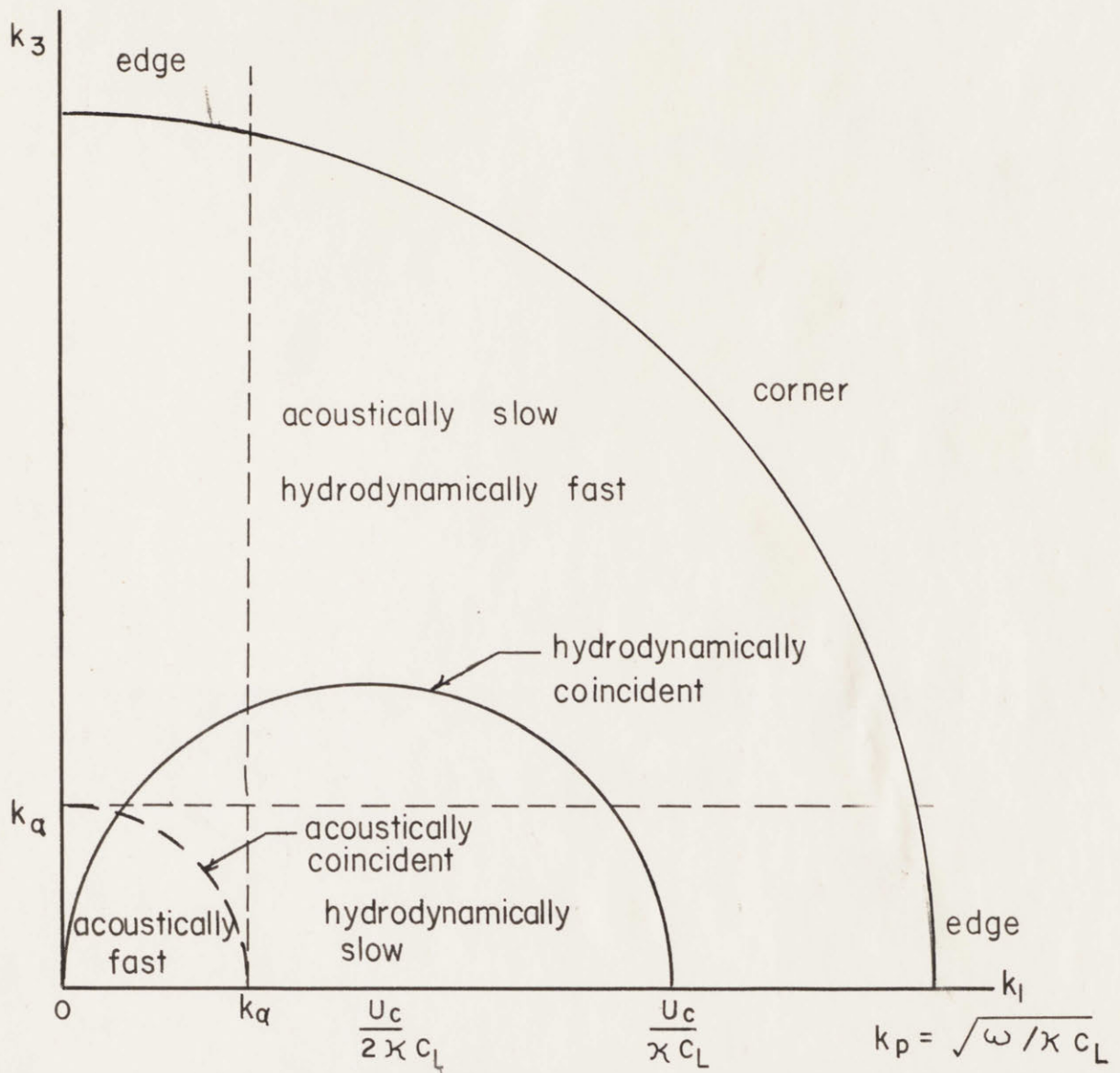


fig. 9 Classification of Plate Modes in Wavenumber Space

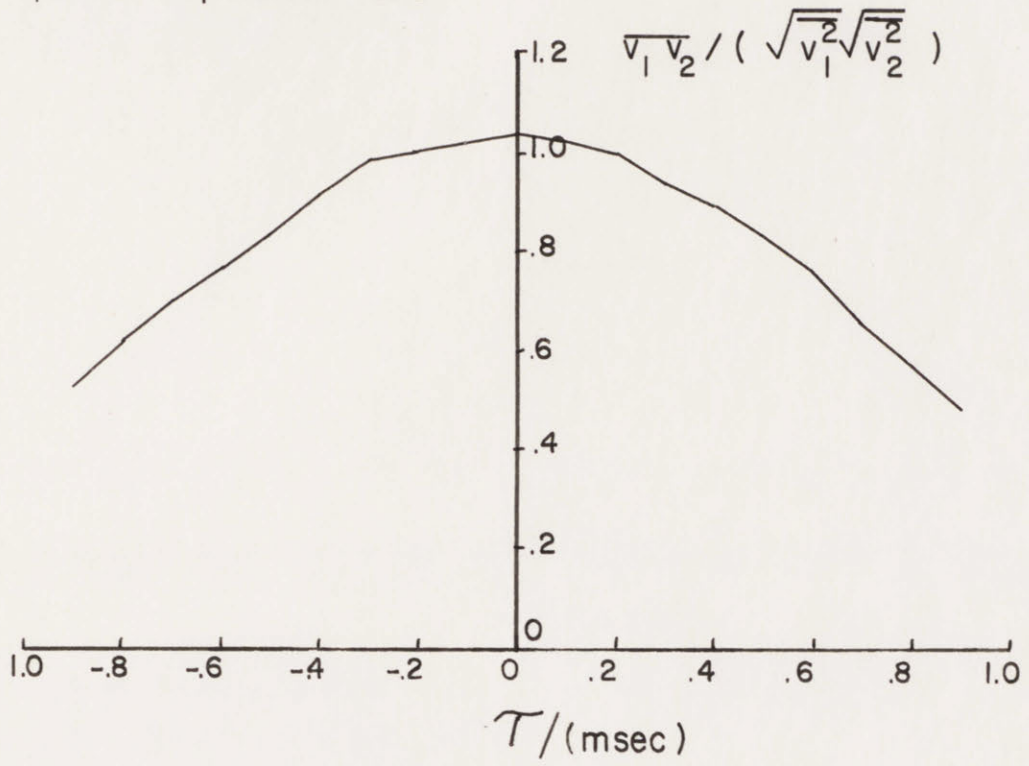
Longitudinal Cross Correlation

Fig. 10a

panel thickness .003"

flow speed 30 m/sec

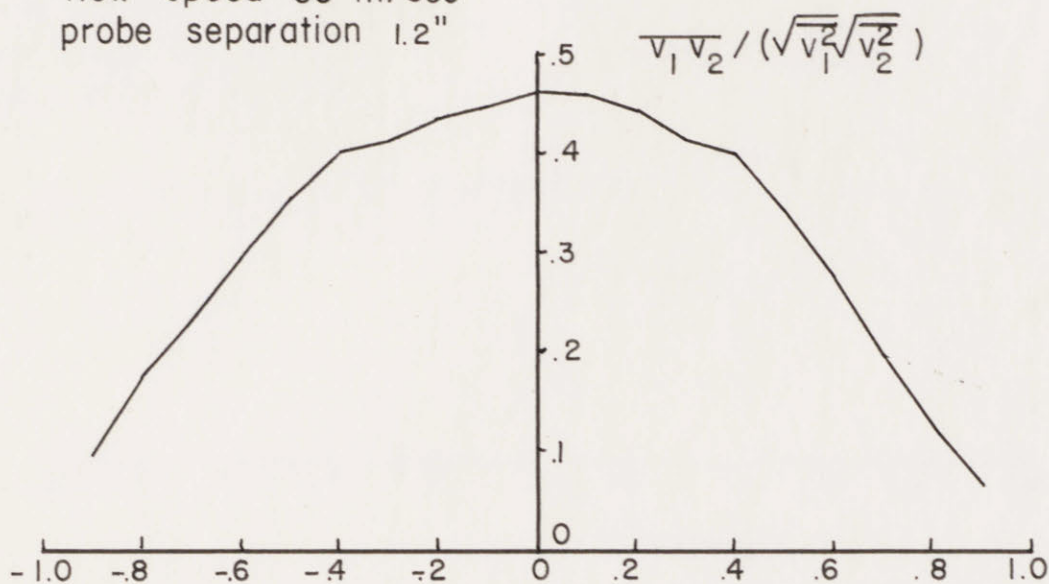
probe separation 3/8"



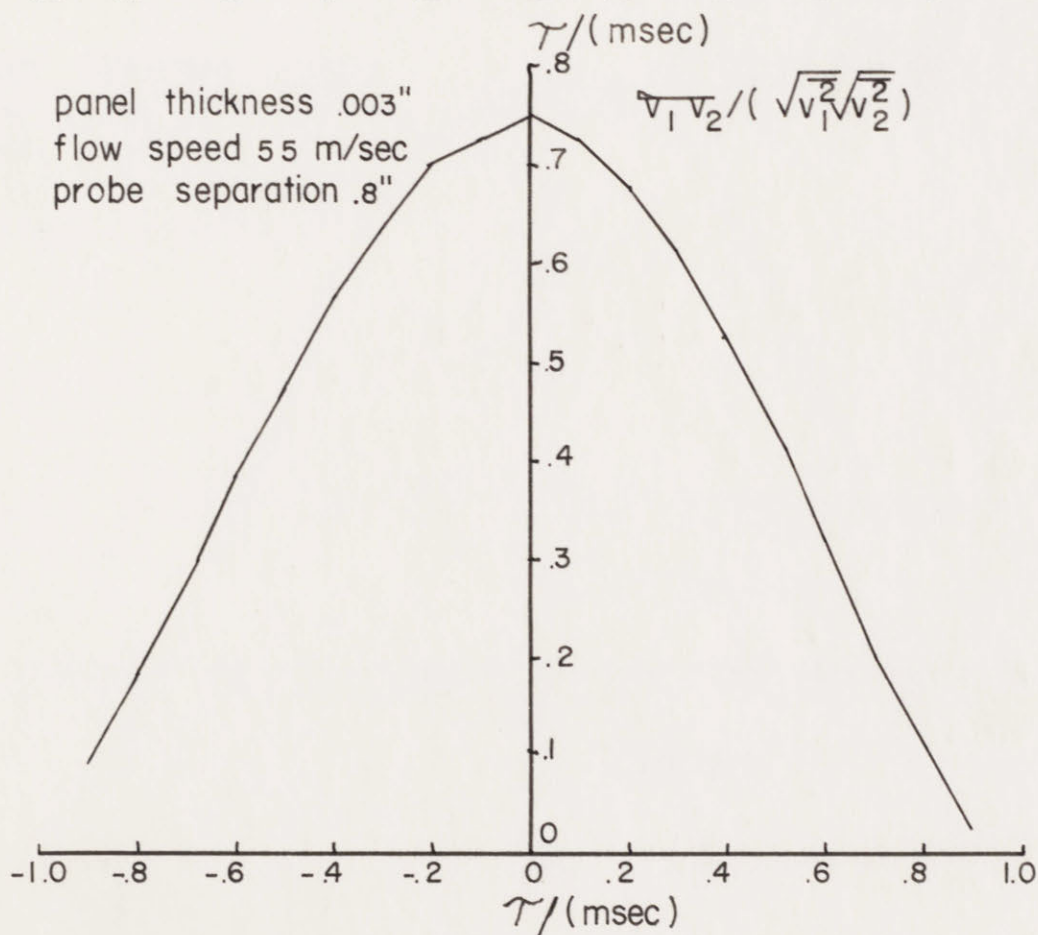
Longitudinal Cross Correlation

Fig. 10 b

panel thickness .003"
 flow speed 55 m/sec
 probe separation 1.2"

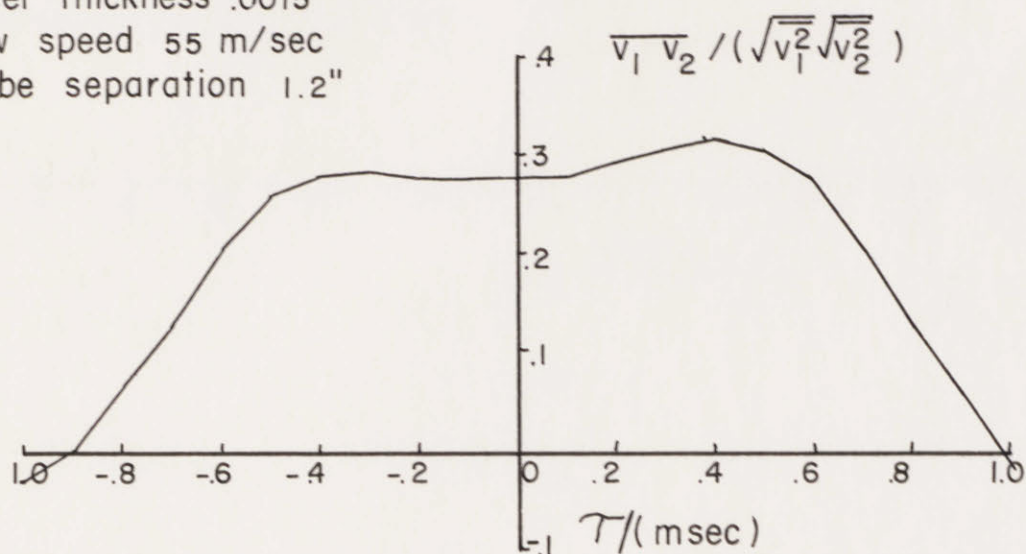


panel thickness .003"
 flow speed 55 m/sec
 probe separation .8"

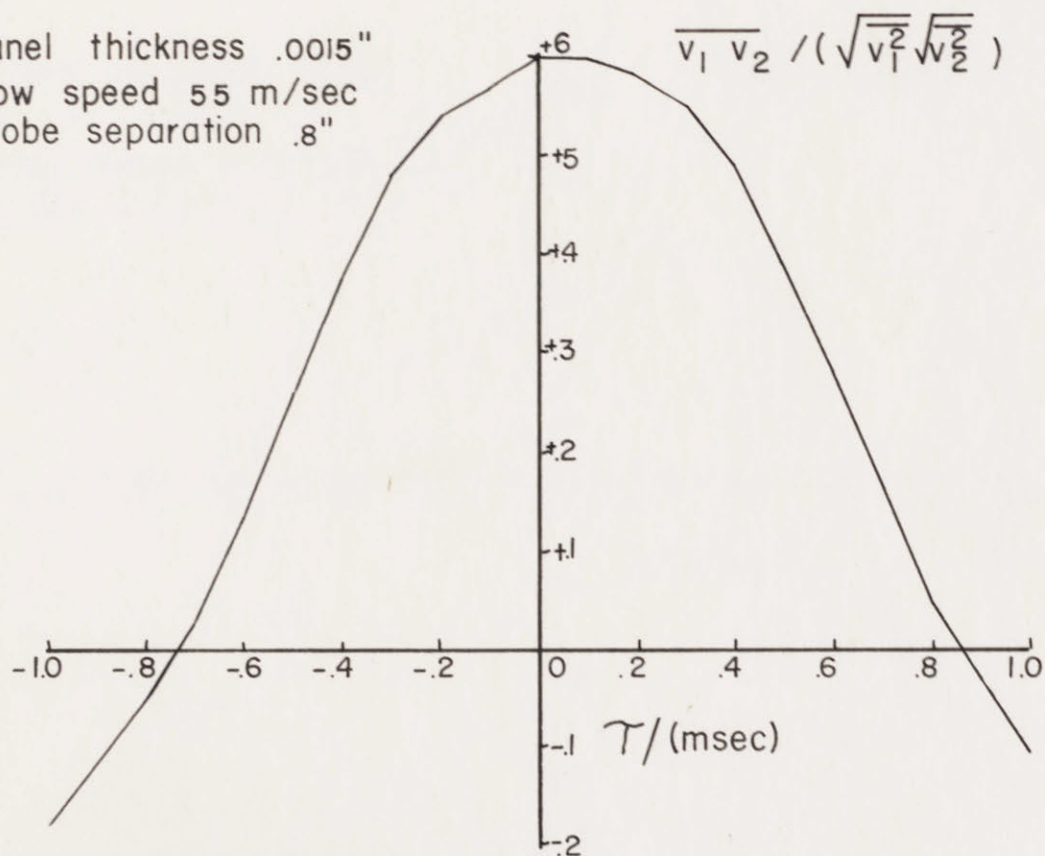


Longitudinal Cross Correlation Fig. 10c

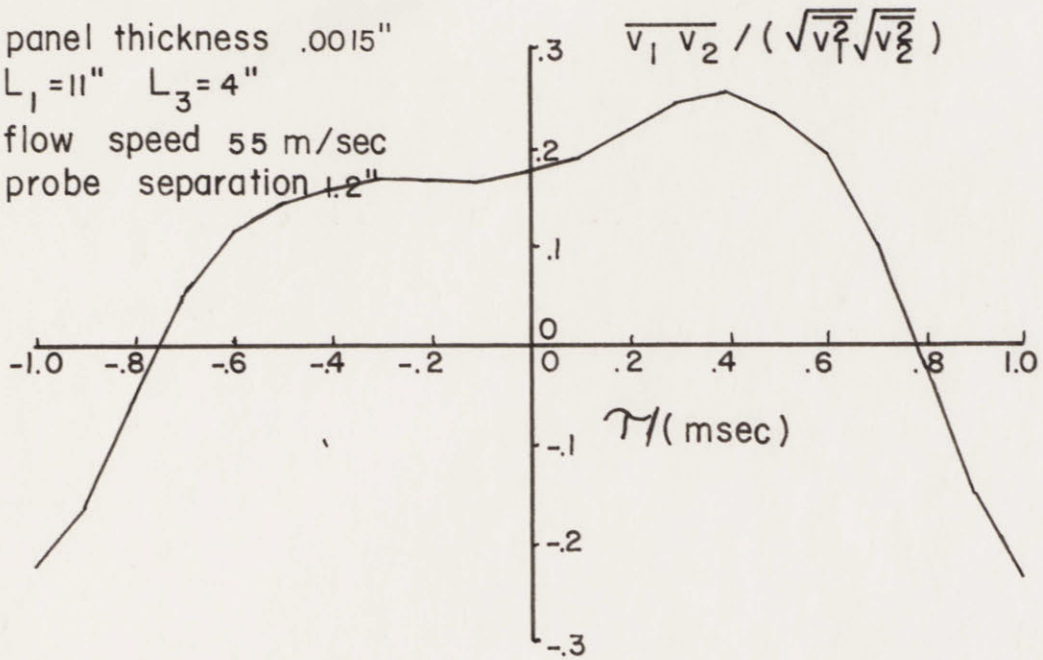
panel thickness .0015"
 flow speed 55 m/sec
 probe separation 1.2"



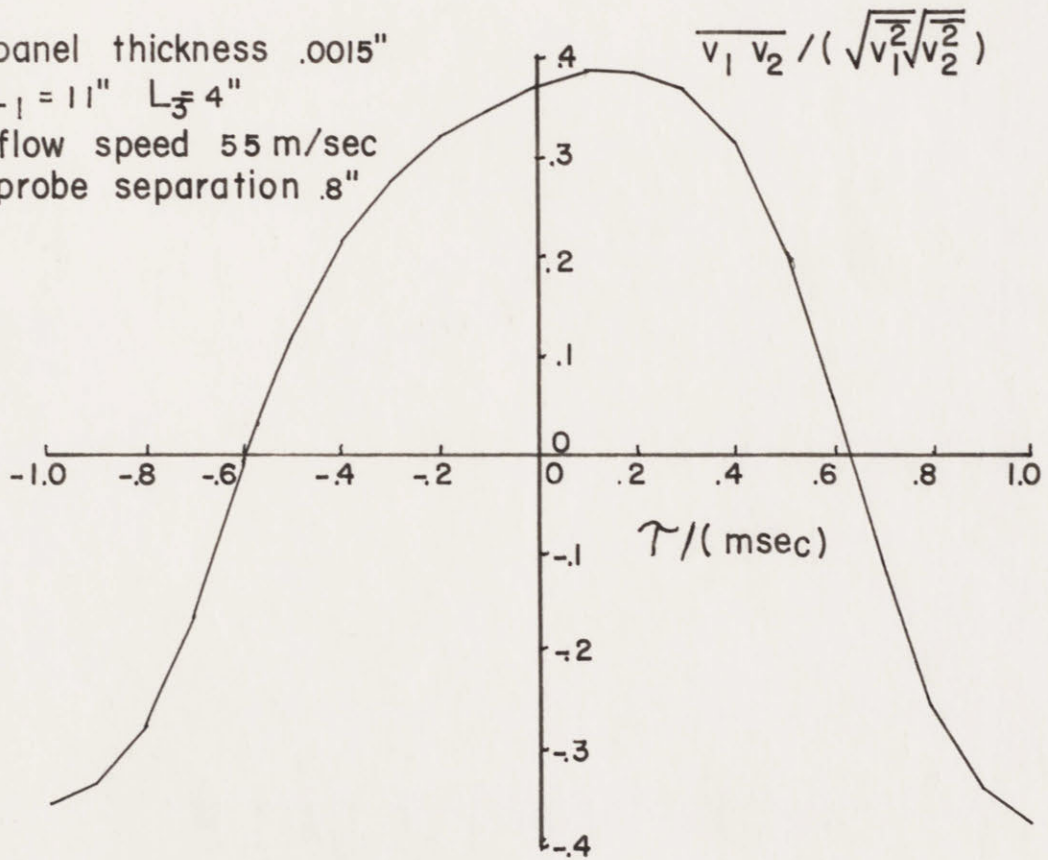
panel thickness .0015"
 flow speed 55 m/sec
 probe separation .8"



panel thickness .0015"
 $L_1 = 11"$ $L_3 = 4"$
 flow speed 55 m/sec
 probe separation 1.2"



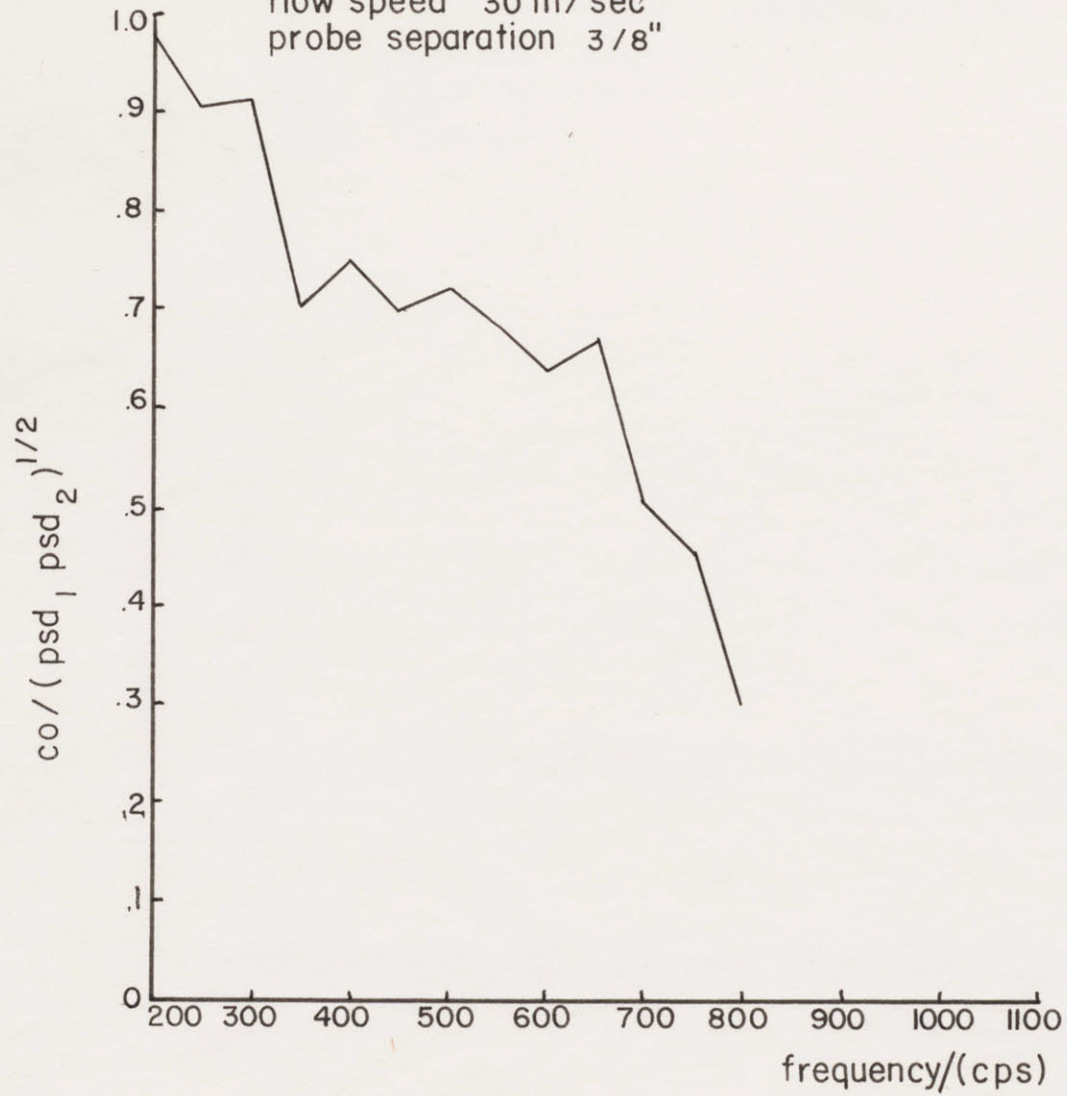
panel thickness .0015"
 $L_1 = 11"$ $L_3 = 4"$
 flow speed 55 m/sec
 probe separation .8"



Cross Spectral Density (co component)

Fig. 11a

panel thickness .006"
flow speed 30 m/sec
probe separation 3/8"

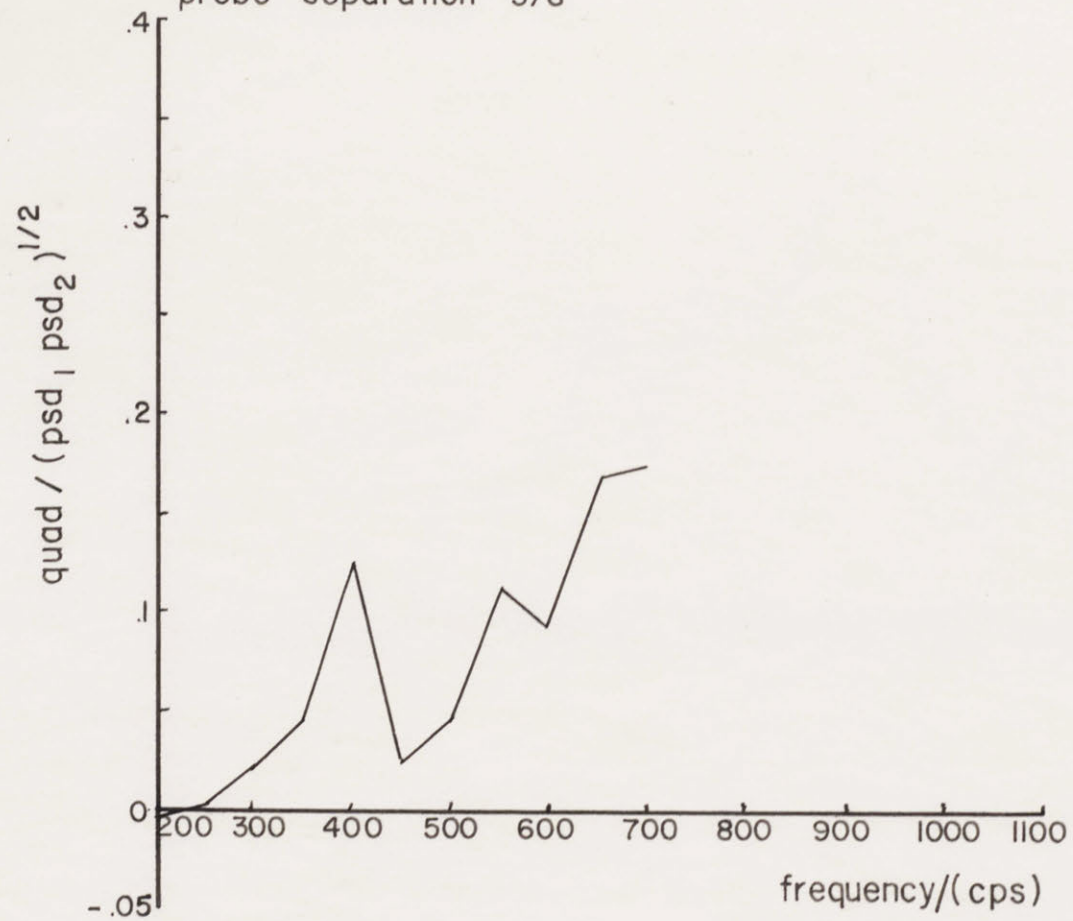


Cross Spectral Density (quad component) Fig. 11 b

panel thickness .006"

flow speed 30 m/sec

probe separation 3/8"



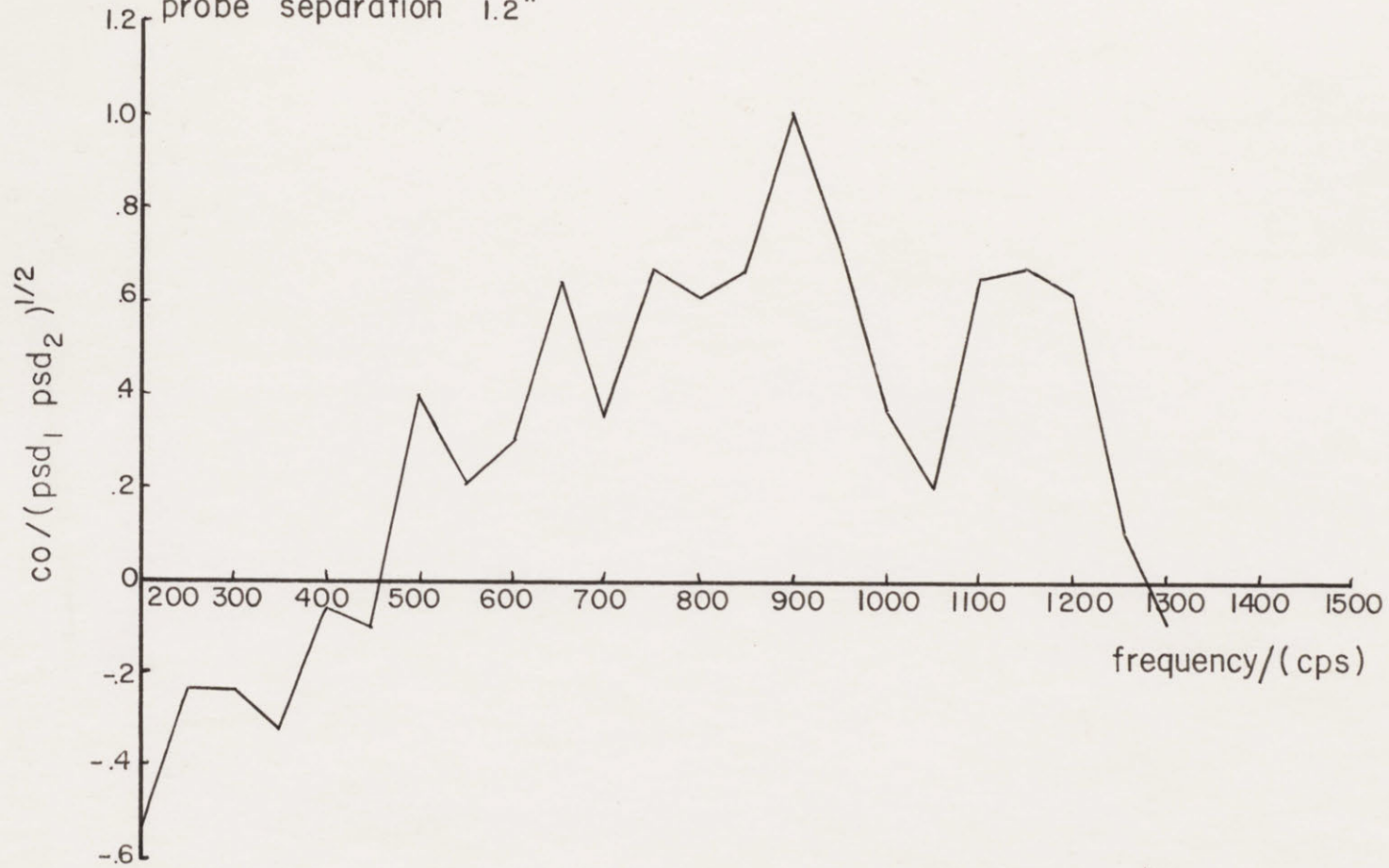
Cross Spectral Density (co component)

Fig. II c

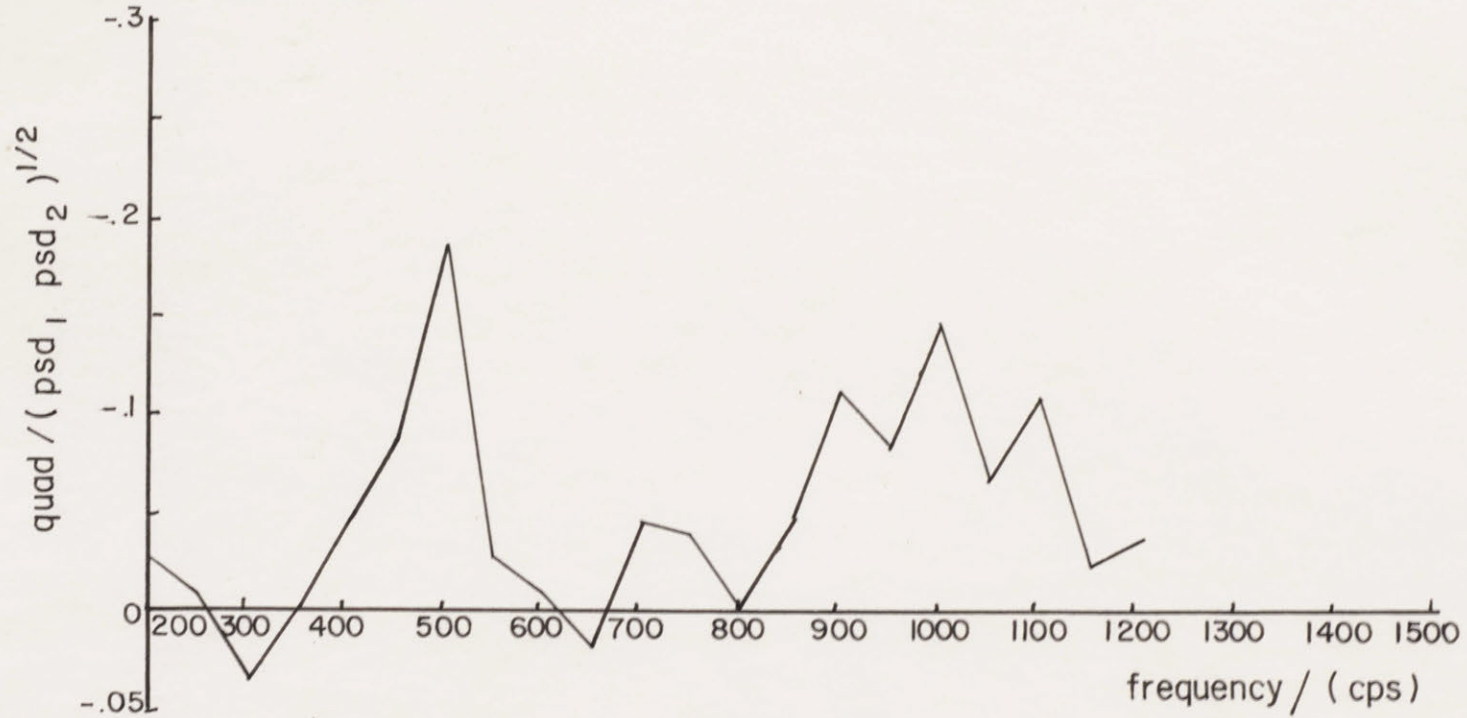
panel thickness .006"

flow speed 55 m/sec

probe separation 1.2"

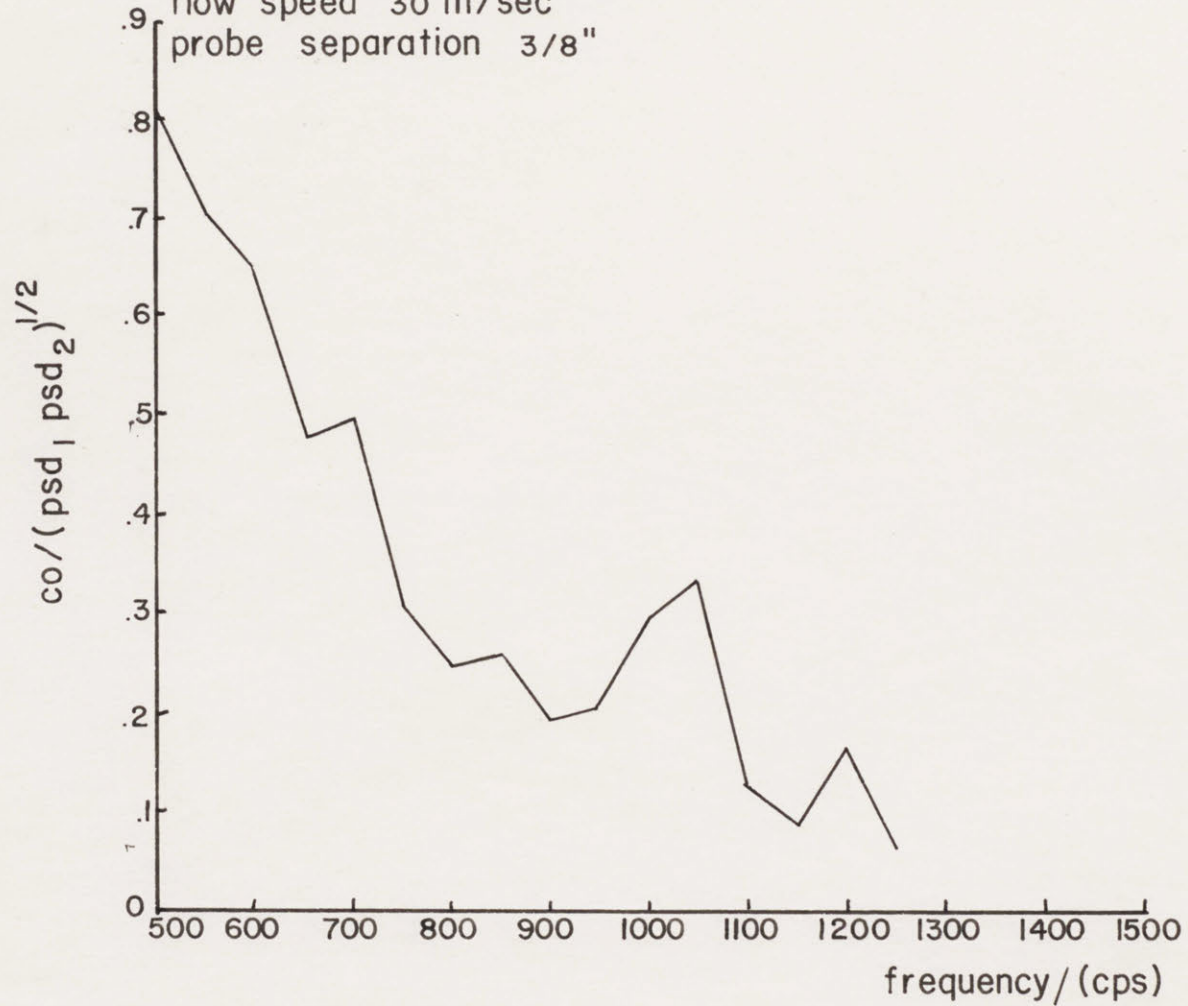


Cross Spectral Density (quad component) Fig. 11d
panel thickness .006"
flow speed 55 m/sec
probe separation 1.2"

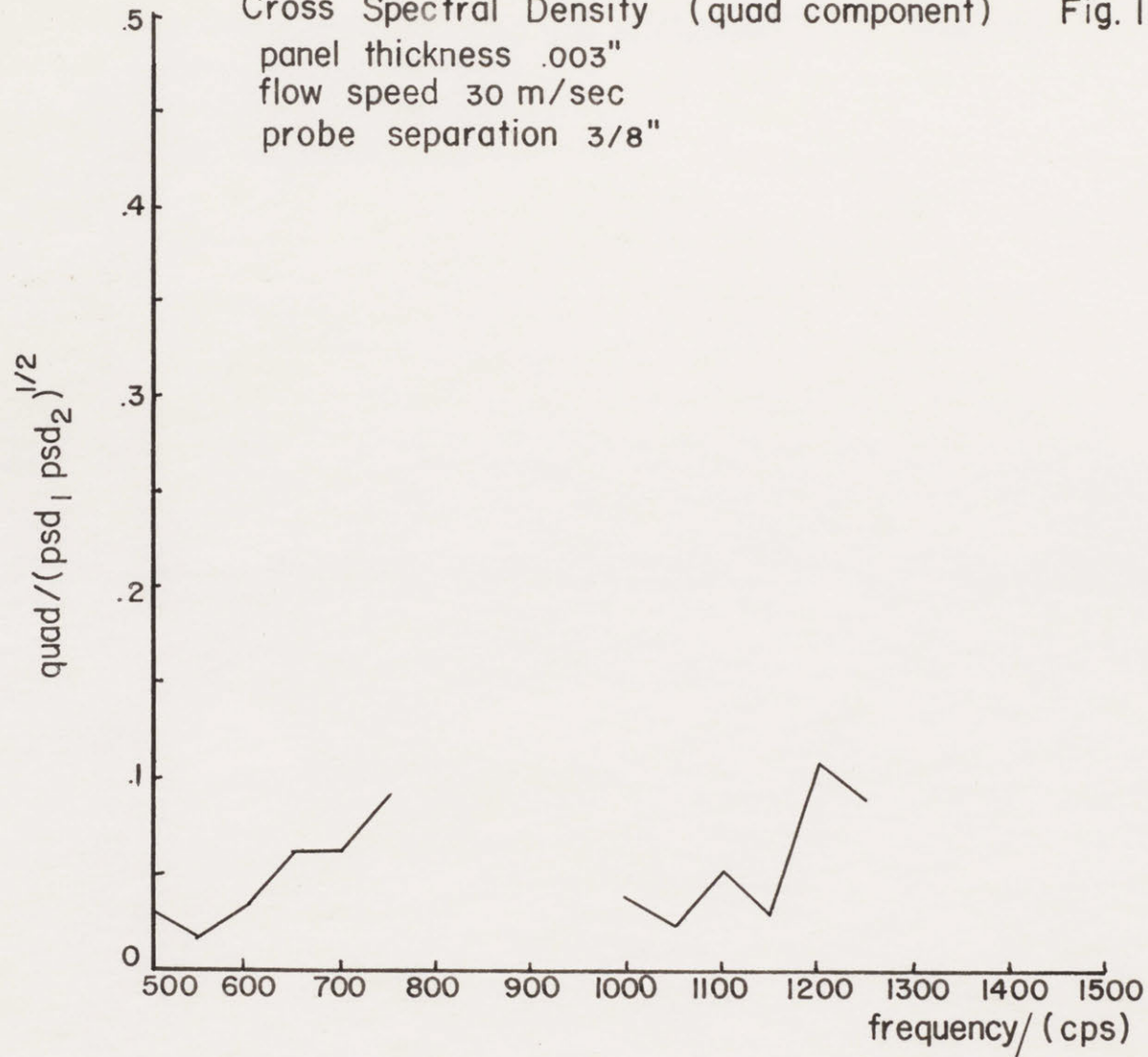


Cross Spectral Density (co component) Fig. 11e

panel thickness .003"
flow speed 30 m/sec
probe separation 3/8"



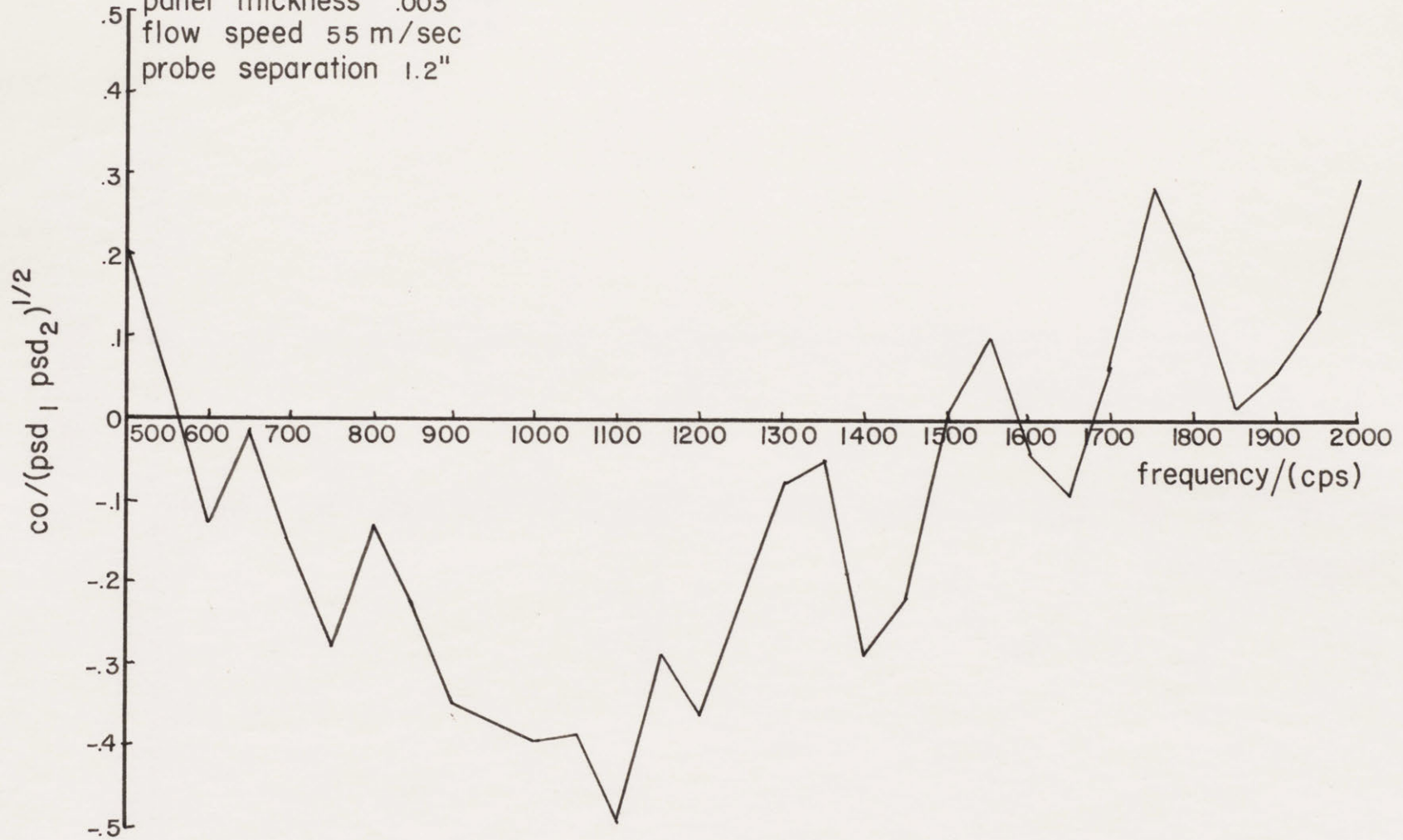
Cross Spectral Density (quad component) Fig. 11f
panel thickness .003"
flow speed 30 m/sec
probe separation 3/8"



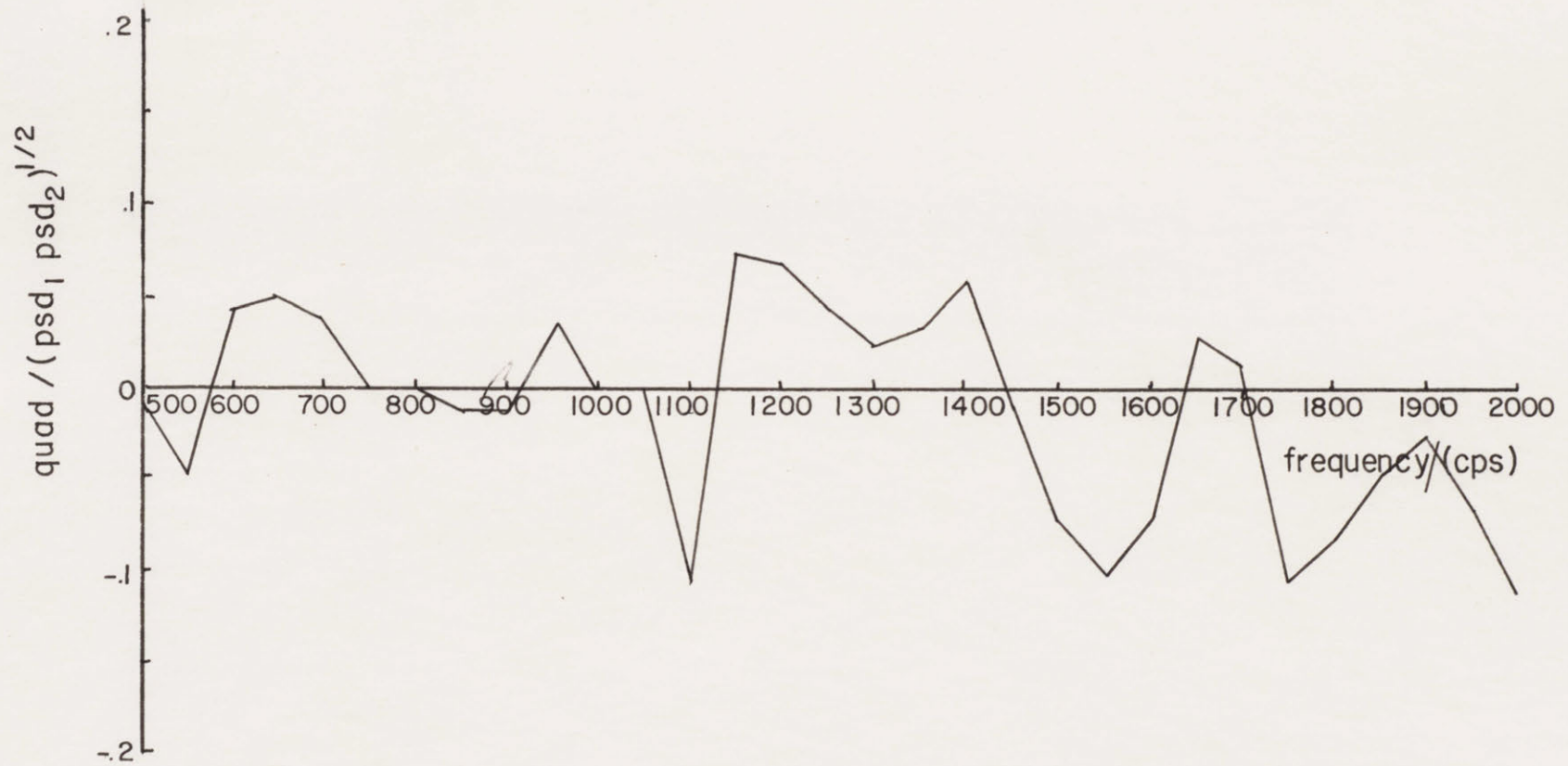
Cross Spectral Density (co component)

Fig. 11g

panel thickness .003"
flow speed 55 m/sec
probe separation 1.2"



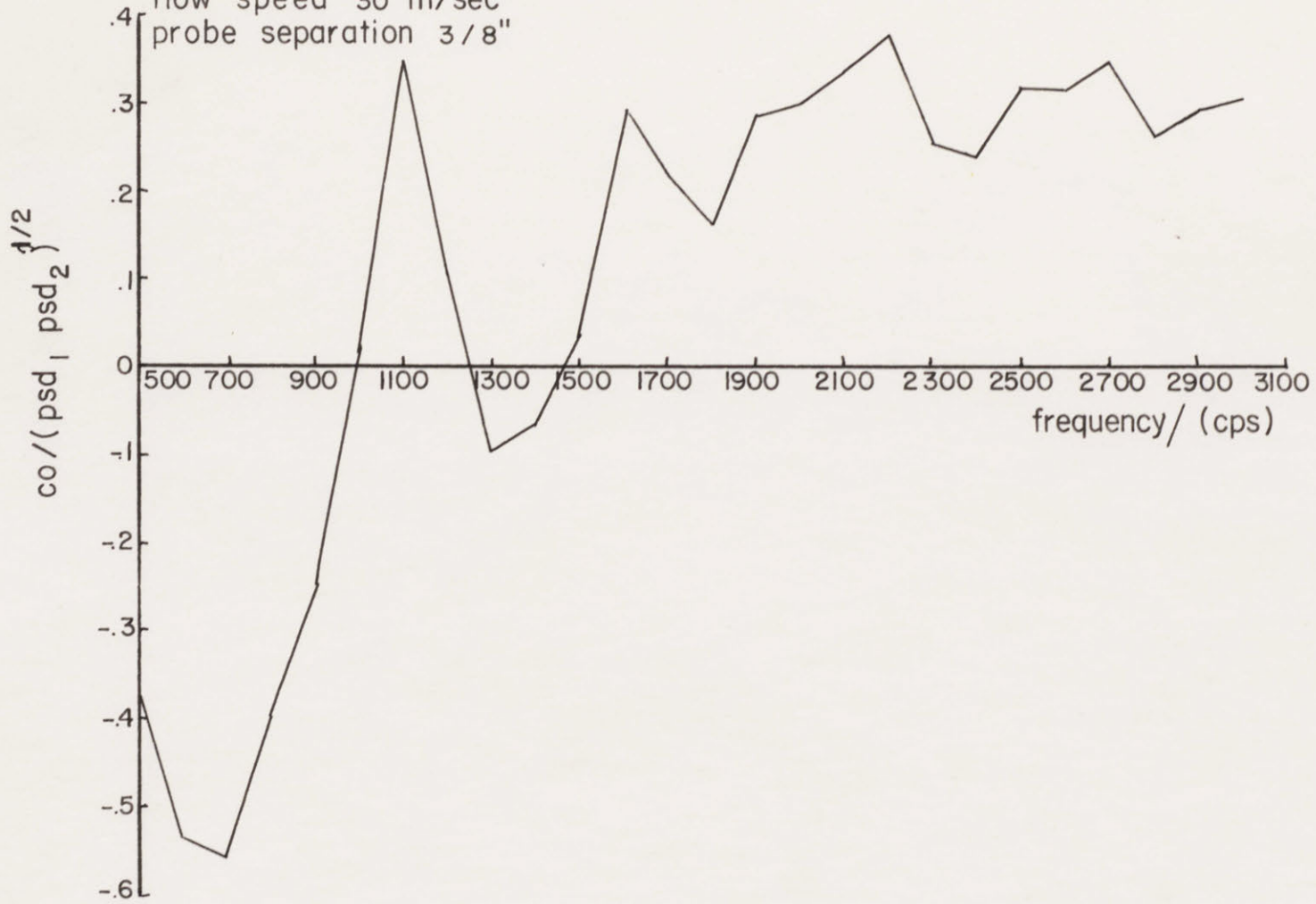
Cross Spectral Density (quad component) Fig. 11h
panel thickness .003"
flow speed 55 m/sec
probe separation 1.2"



Cross Spectral Density (co. component)

Fig. II i

panel thickness .0015"
flow speed 30 m/sec
probe separation 3/8"

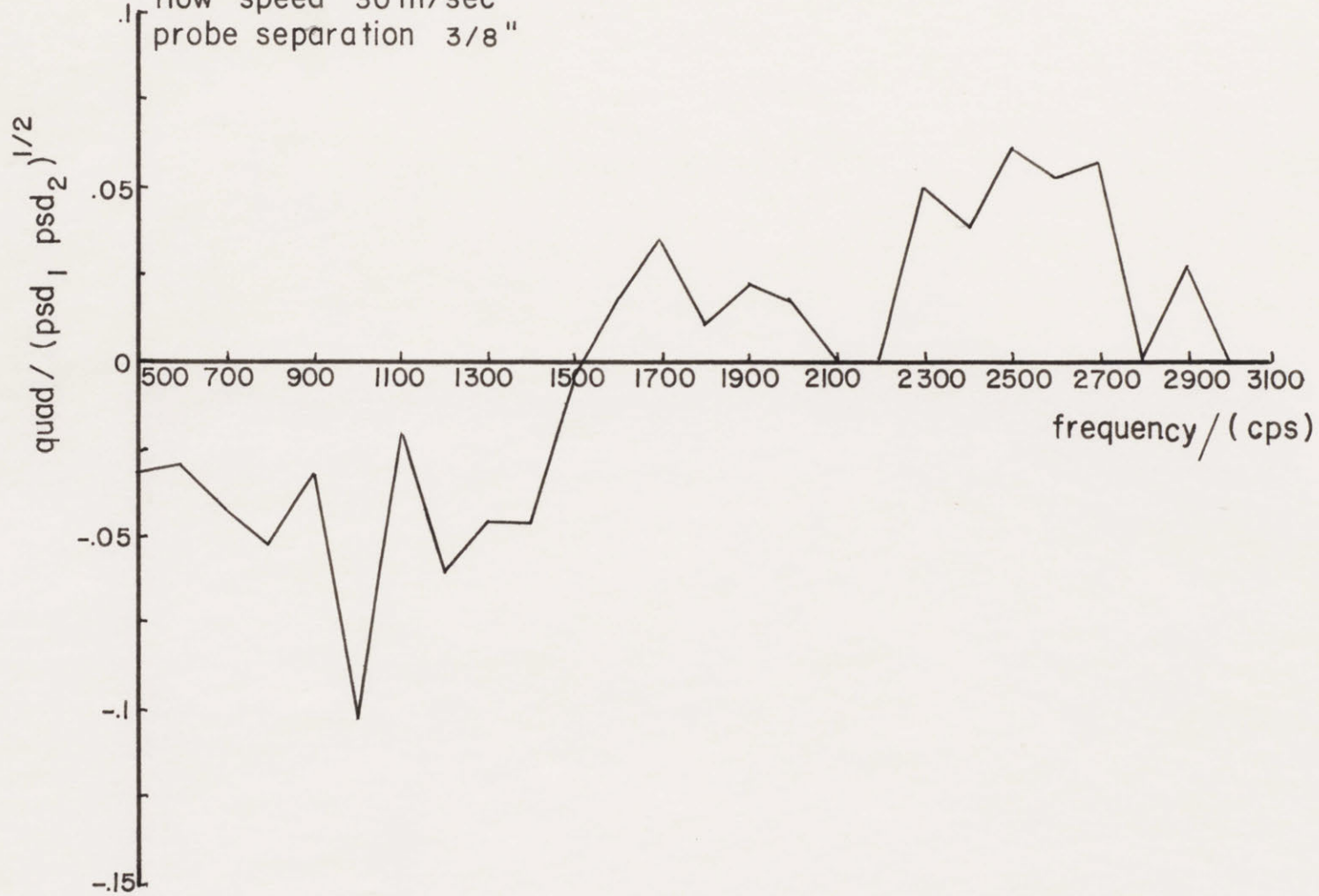


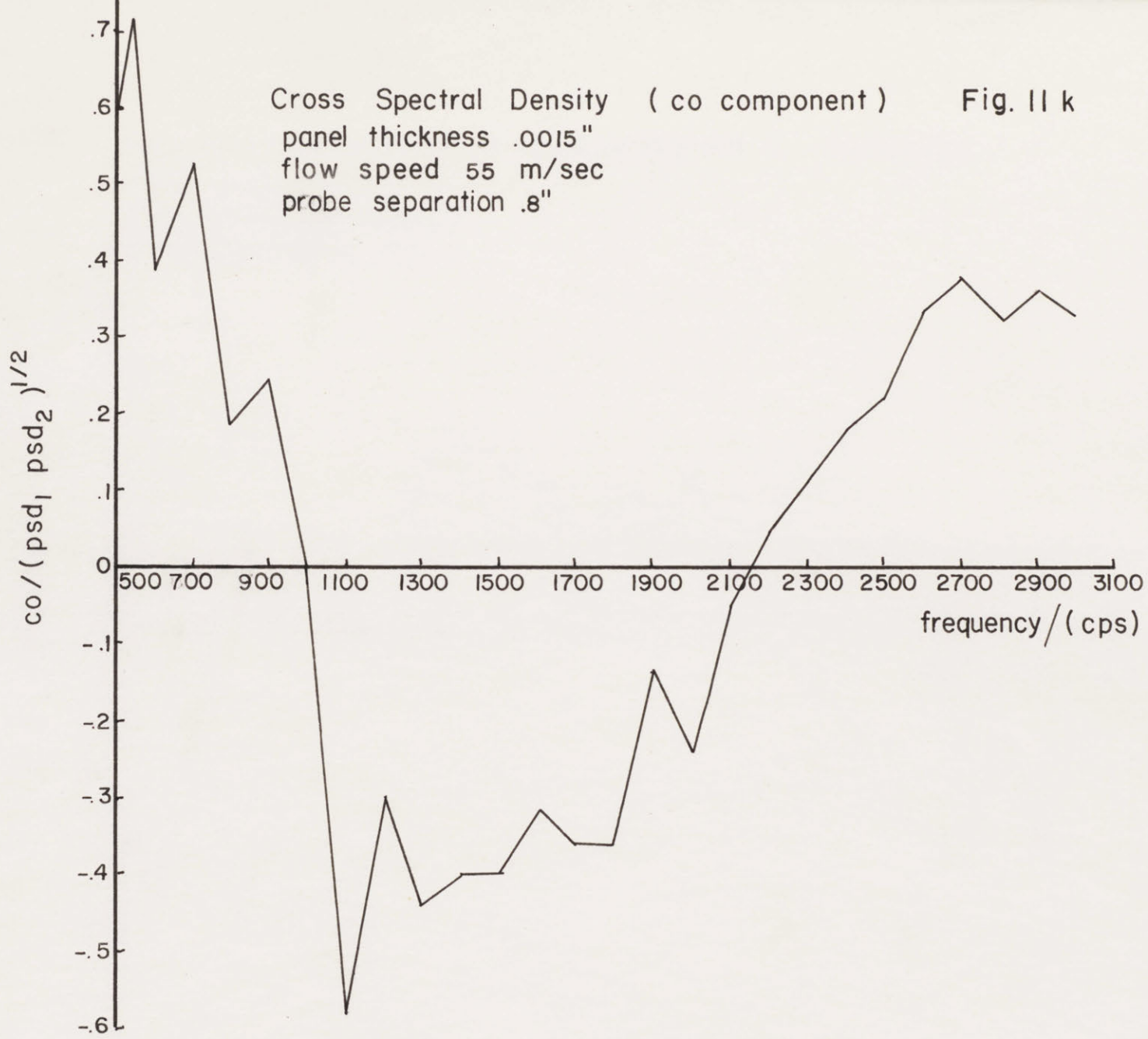
Cross Spectral Density (quad component) Fig. 11j

panel thickness .0015"

flow speed 30 m/sec

probe separation 3/8"





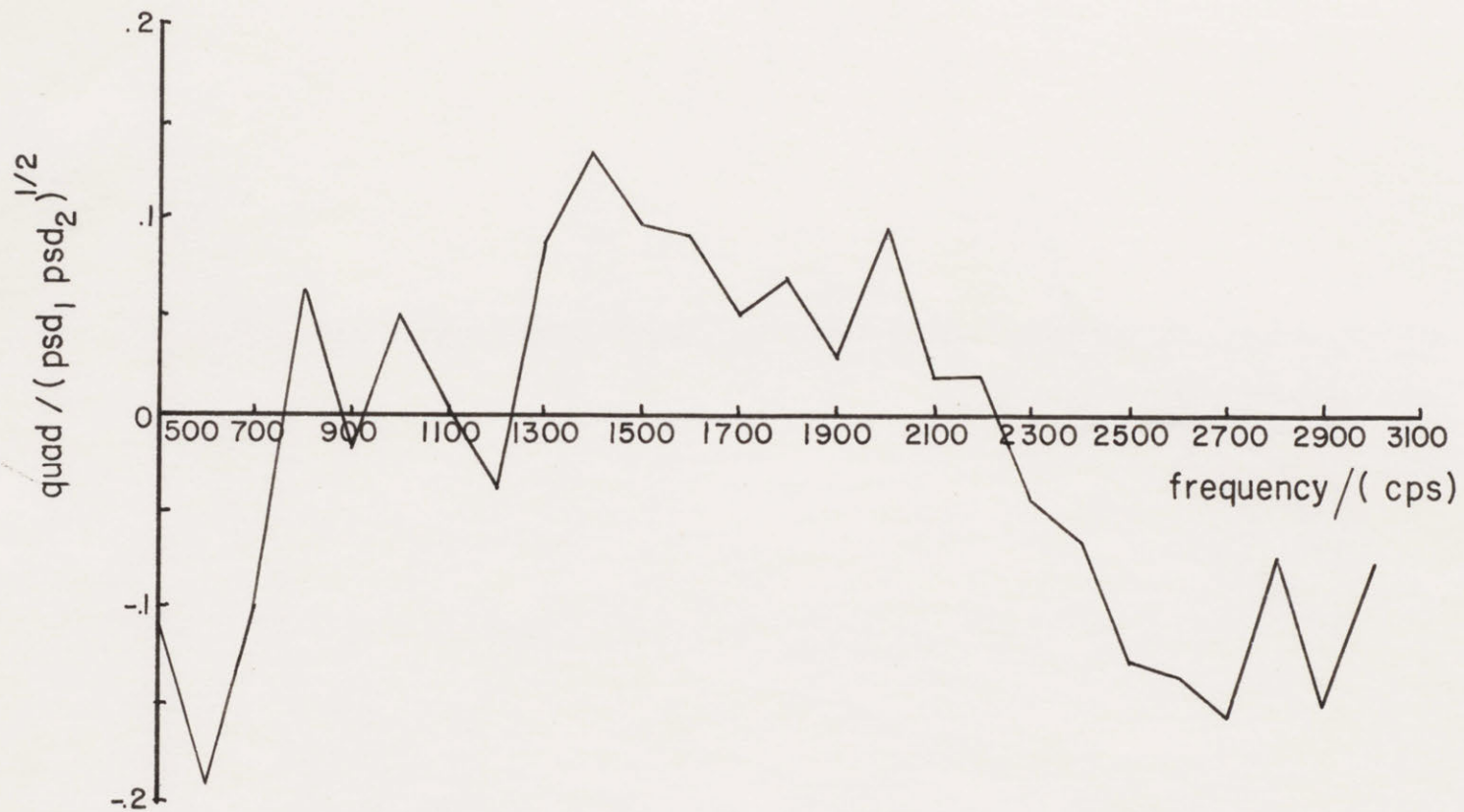
Cross Spectral Density (quad component)

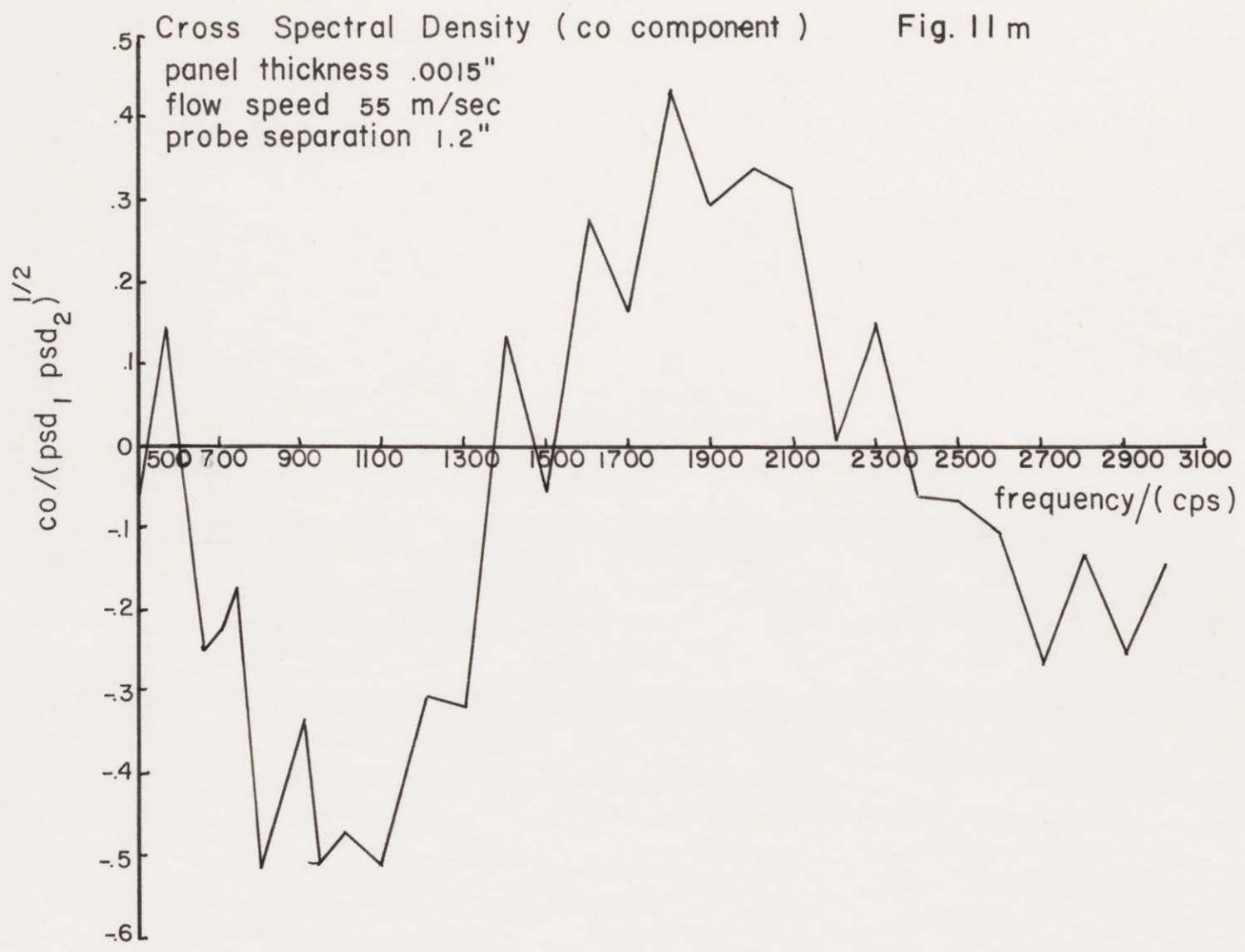
Fig. II L

panel thickness .0015"

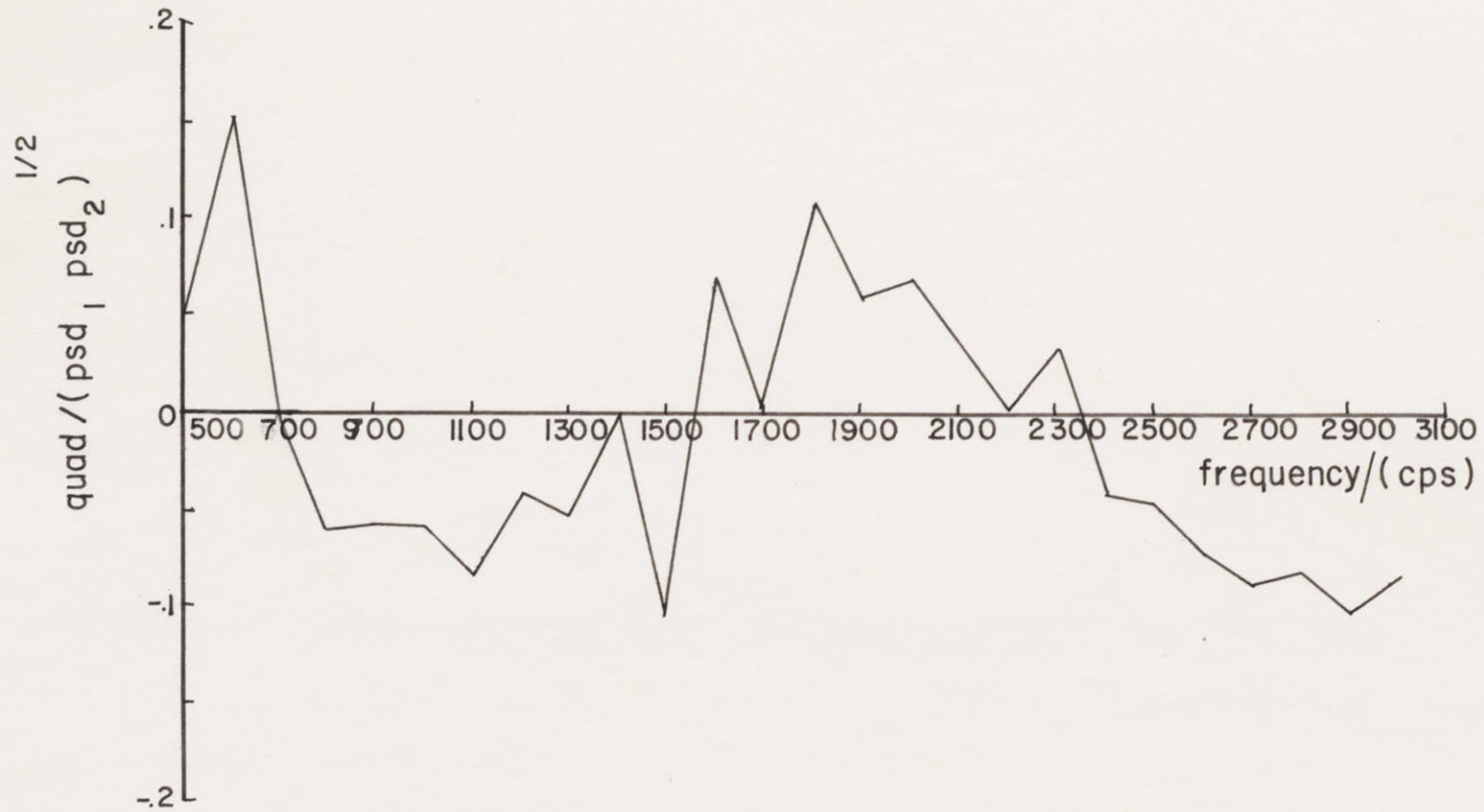
flow speed 55 m/sec

probe separation .8"



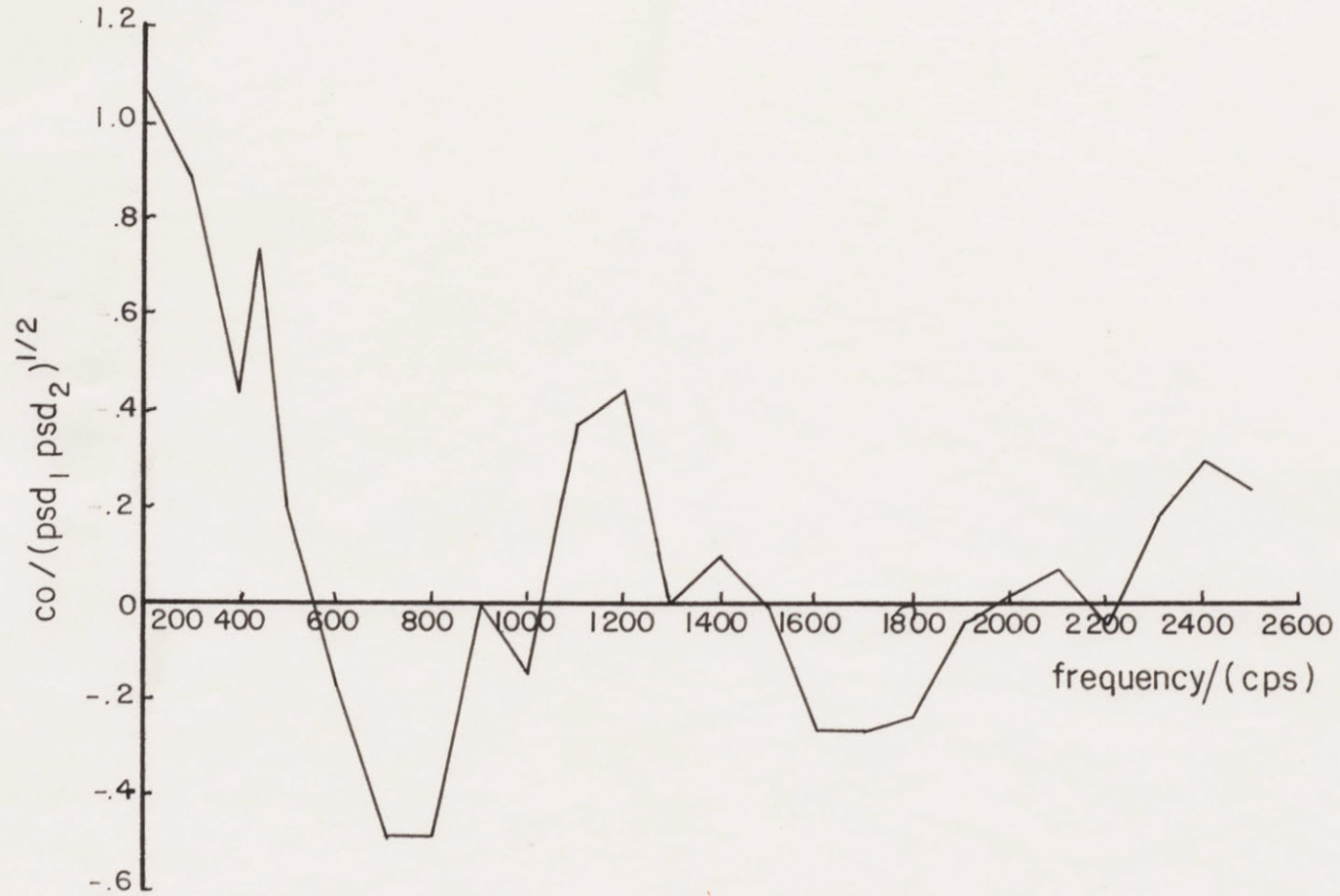


Cross Spectral Density (quad component) Fig. 11 n
panel thickness .0015"
flow speed 55 m/sec
probe separation 1.2"



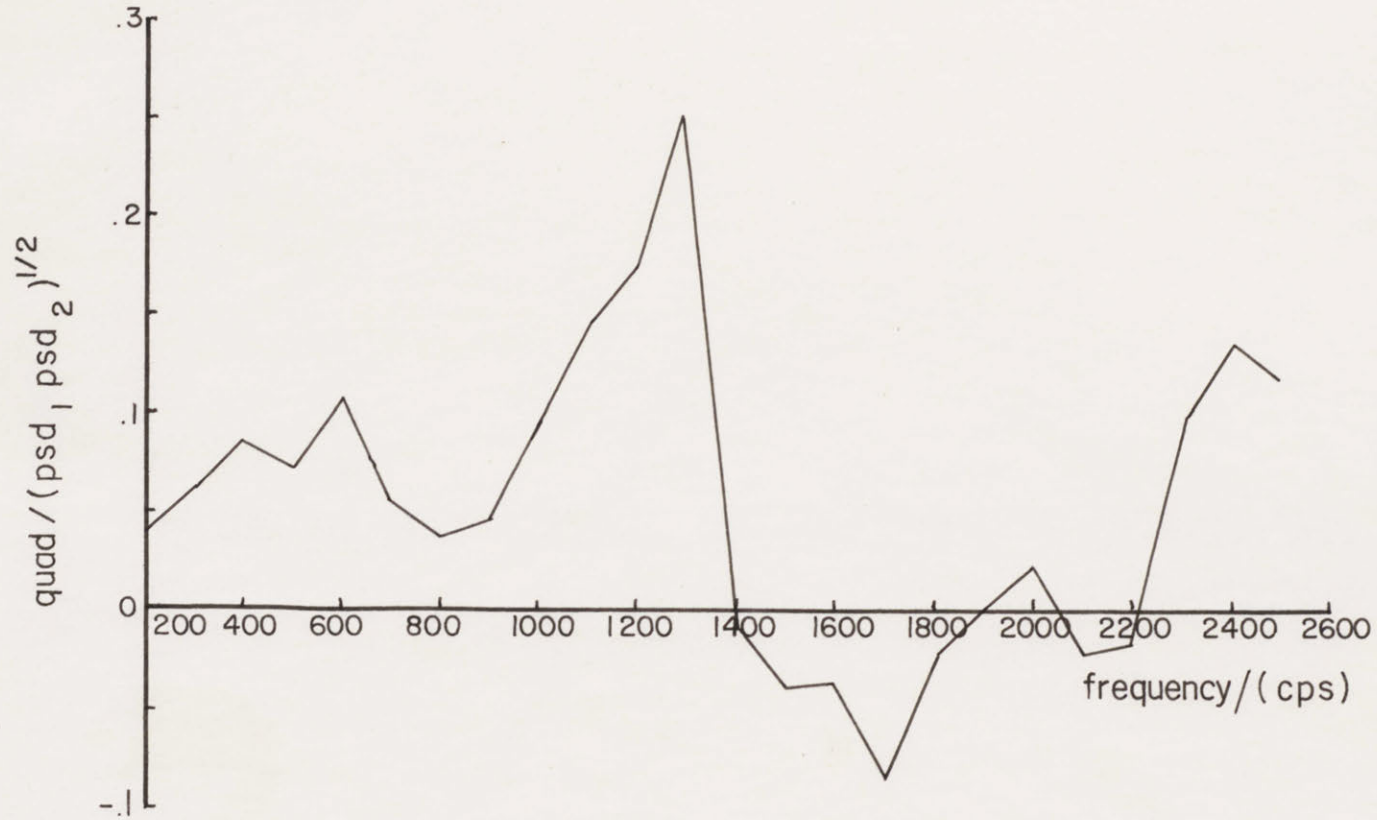
Cross Spectral Density (co component)
panel .thickness .0015" length 11" width 4"
flow speed 45 m/sec
probe separation 1.2"

Fig. II o



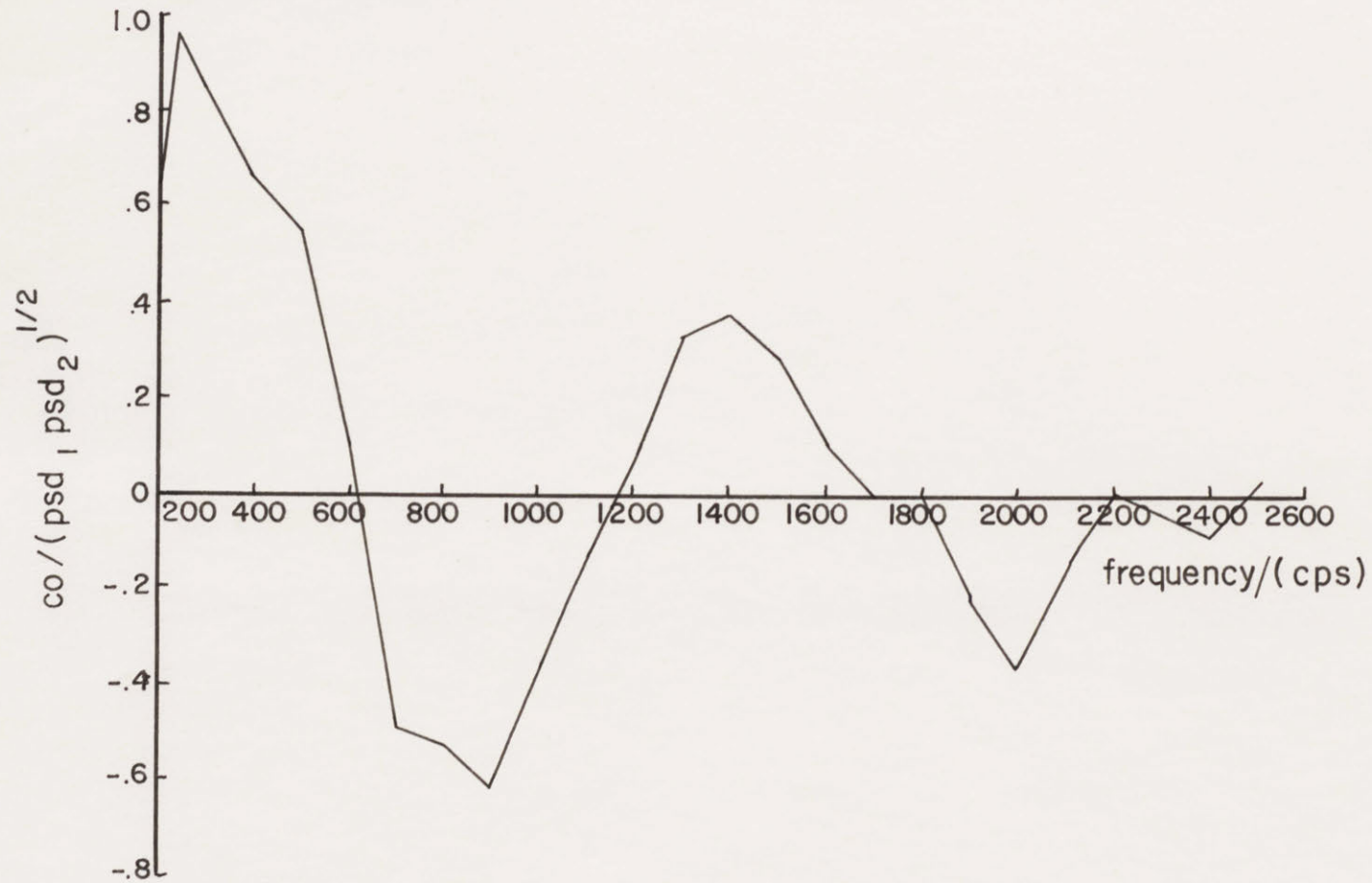
Cross Spectral Density (quad component)
panel thickness .0015" length 11" width 4"
flow speed 45 m/sec
probe separation 1.2"

Fig. 11p



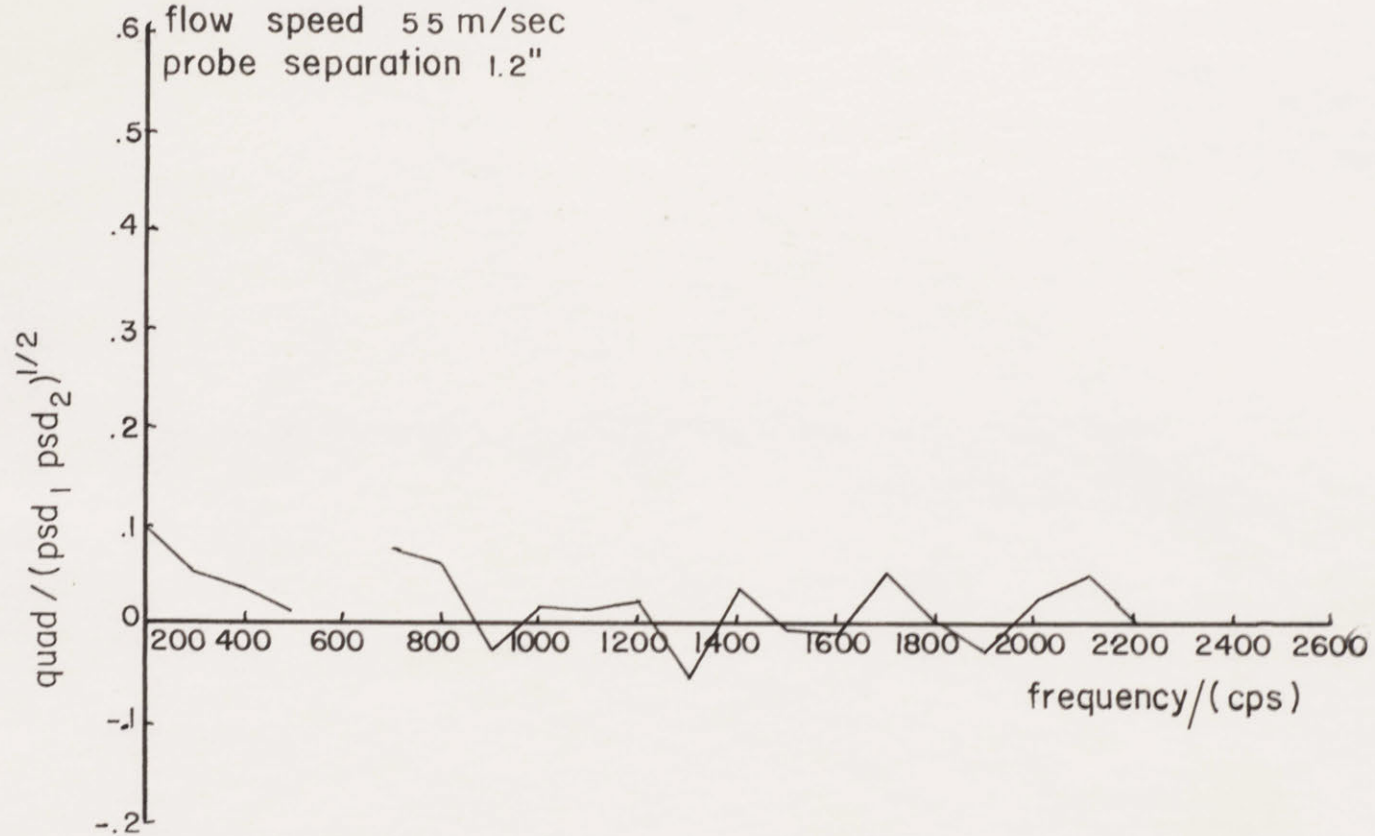
Cross Spectral Density (co component)
panel thickness .0015" length 11" width 4"
flow speed 55 m/sec
probe separation 1.2"

Fig. 11q



Cross Spectral Density (quad component)
panel thickness .0015" length 11" width 4"
flow speed 55 m/sec
probe separation 1.2"

Fig. 11r



Narrow Band Cross Correlation

Fig. 12 a

panel thickness .003"

flow speed 55 m/sec $\omega_0 = 1400$ cps

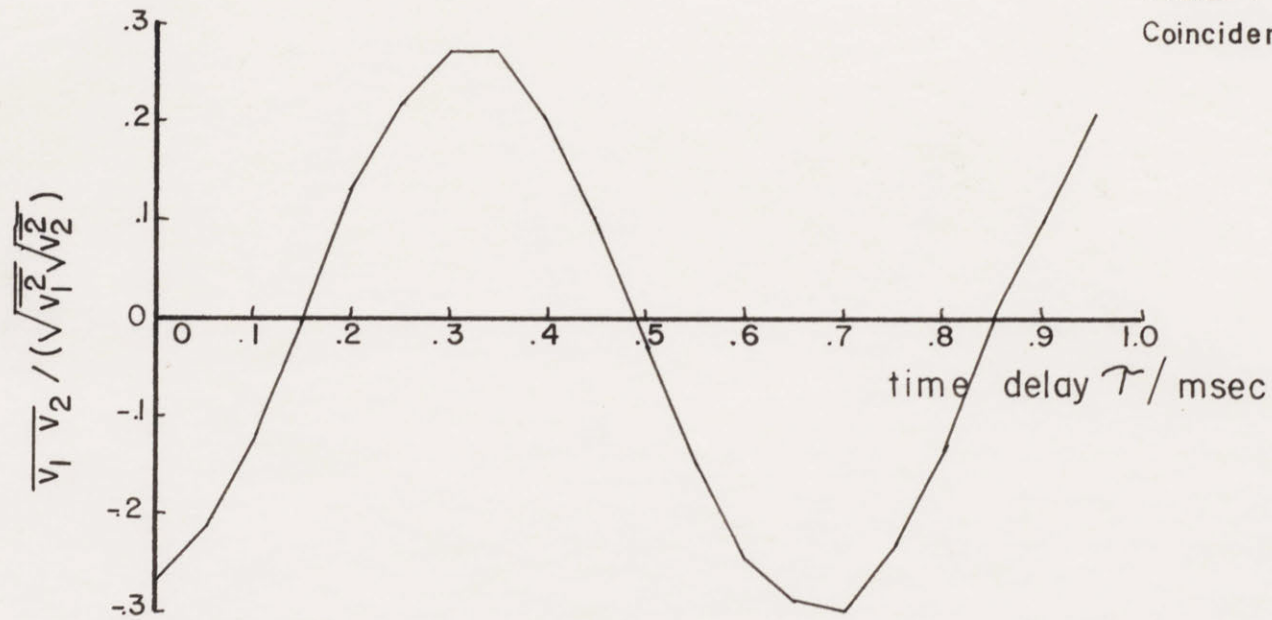
probe separation 1.2" $\Delta\omega = 50$ cps

Quadrature spectral point

occurs at $\tau = .1785$

value = .0698

Coincidence spectral value = -.261



Narrow Band Cross Correlation

Fig. 12 b

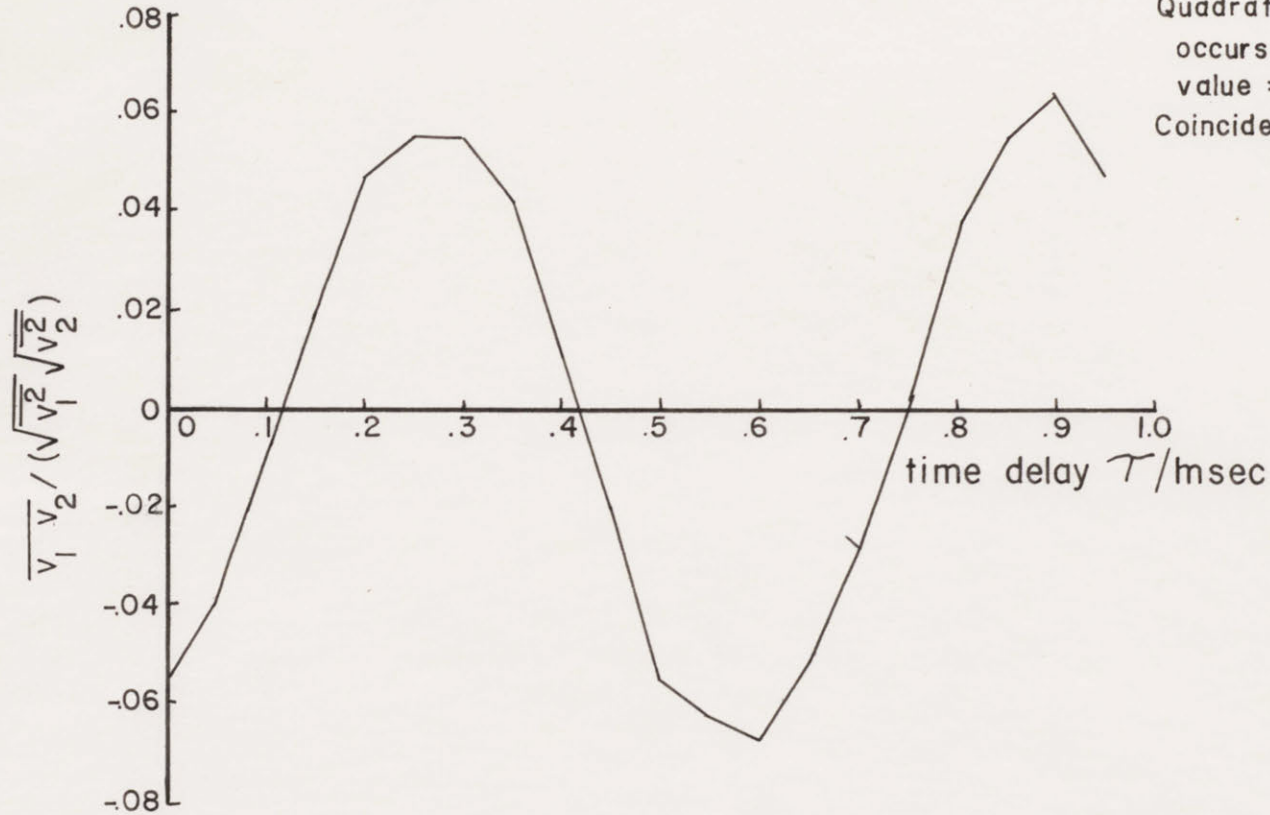
panel thickness .003"

flow speed 55 m/sec

probe separation 1.2"

$\omega_0 = 1600$ cps

$\Delta\omega = 50$ cps



Narrow Band Cross Correlation Fig.12c

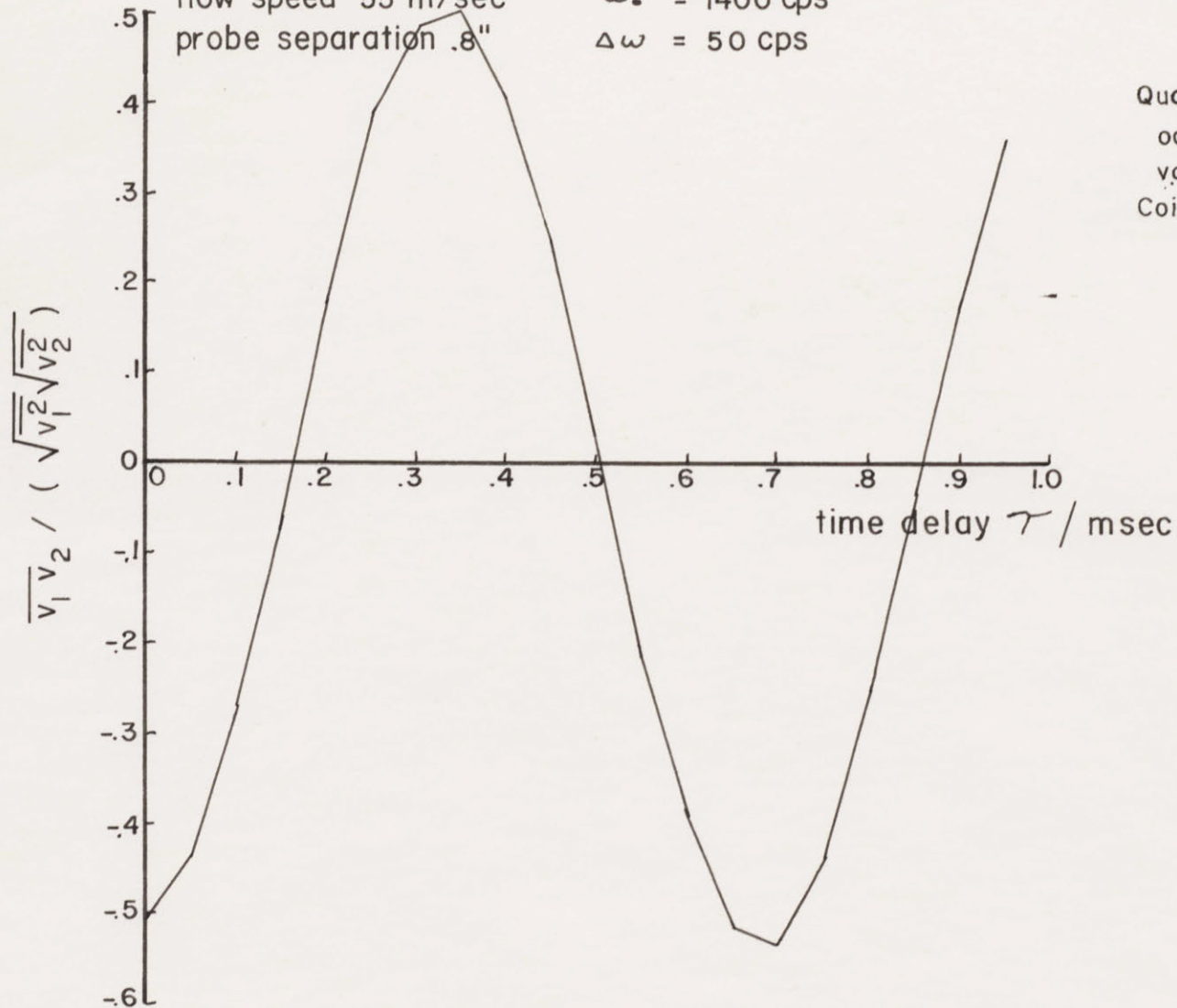
panel thickness .0015"

flow speed 55 m/sec

probe separation .8"

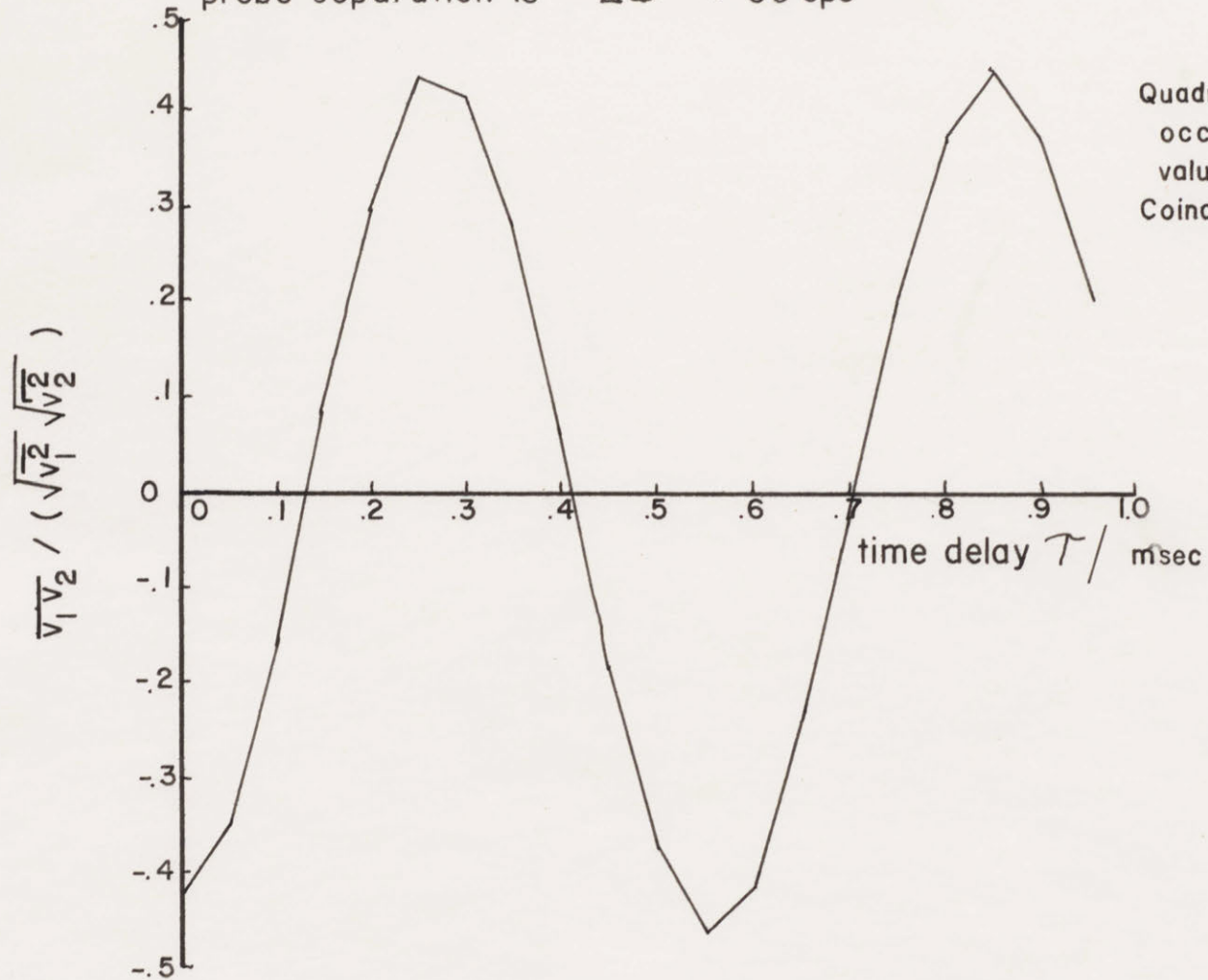
$\omega_c = 1400$ cps

$\Delta\omega = 50$ cps



Quadrature spectral point
occurs at $\tau = .1785$ msec
value = .0805
Coincidence spectral value = -.5

Narrow Band Cross Correlation Fig. 12 d
panel thickness .0015"
flow speed 55 m/sec $\omega_c = 1700$ cps
probe separation .8" $\Delta\omega = 50$ cps



Narrow Band Cross Correlation Fig. 12e

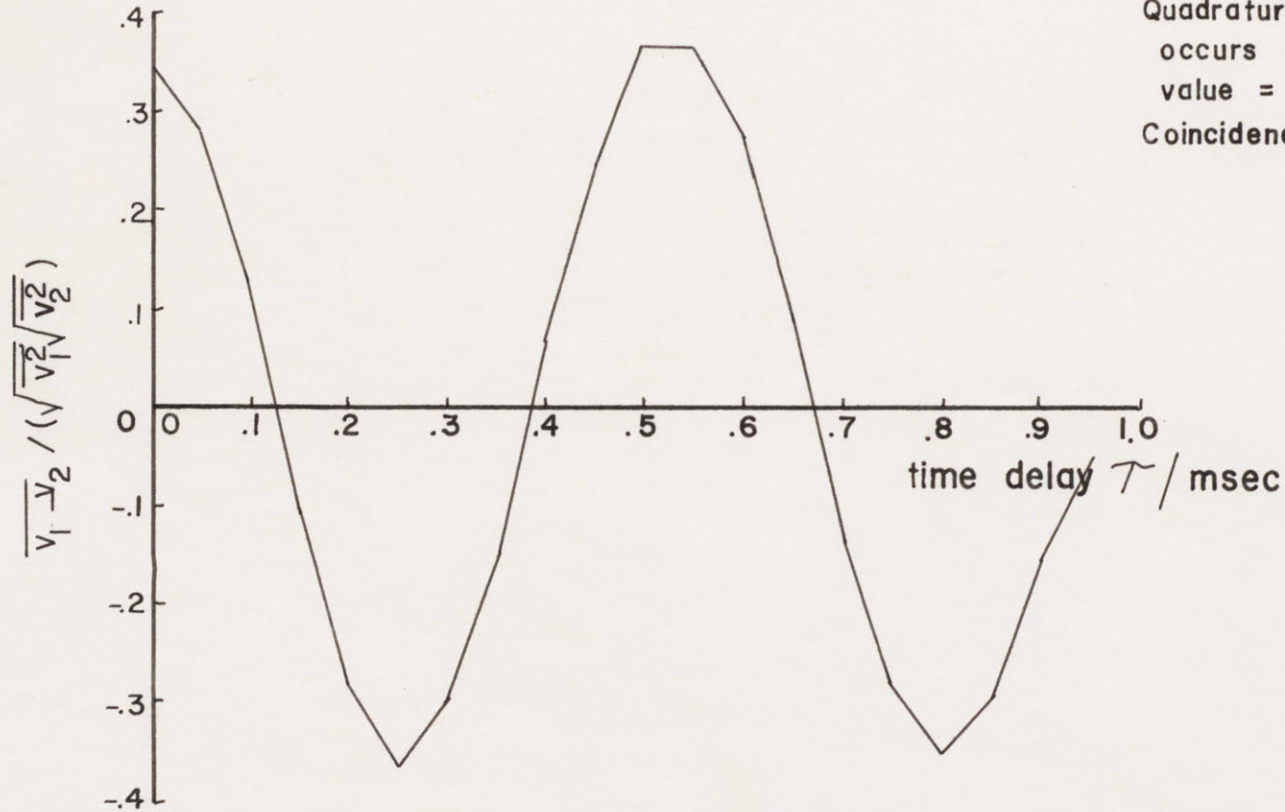
panel thickness .0015"

flow speed 55 m/sec

probe separation 1.2

$\omega_0 = 1800$ cps

$\Delta\omega = 50$ cps



Quadrature spectral point
occurs at $\tau = .139$ msec
value = $-.0524$

Coincidence spectral value = .35

Figure (13)

Broadband Vibration Levels

Panel Thickness .006"

Flow Speed	Mean Square Displacement
30 m/sec	$6.93 \times 10^{-8} \text{ in}^2$
45 m/sec	$4.14 \times 10^{-7} \text{ in}^2$
55 m/sec	$4.33 \times 10^{-7} \text{ in}^2$

Panel Thickness .003"

Flow Speed	Mean Square Displacement
30 m/sec	$1.76 \times 10^{-7} \text{ in}^2$
45 m/sec	$2.20 \times 10^{-7} \text{ in}^2$
55 m/sec	$2.86 \times 10^{-7} \text{ in}^2$

Panel Thickness .0015"

Flow Speed	Mean Square Displacement
20 m/sec	$2.61 \times 10^{-7} \text{ in}^2$
45 m/sec	$4.07 \times 10^{-7} \text{ in}^2$
55 m/sec	$3.28 \times 10^{-7} \text{ in}^2$